Evidence for microbial iron reduction in the methanic sediments of the oligotrophic SE Mediterranean continental shelf

Hanni Vigderovich[1], Lewen Liang[2], Barak Herut[3], Fengping Wang[2], Eyal Wurgaft[1,4], Maxim Rubin-Blum[3] and Orit Sivan[1]

[1]The Department of Geological and Environmental Sciences, Ben-Gurion University of the Negev, Beer-Sheva, 8410501, Israel.
[2] School of Life Sciences and Biotechnology, Shanghai JiaoTong University, Shanghai, 200240, P.R.China.
[3] Israel Oceanographic and Limnological Research, Haifa, 31080, Israel.
[4]Currently: The Department of Marine Chemistry and Biochemistry, Woods-Hole Oceanographic Institution, Woods-Hole, USA
Correspondence to: Orit Sivan (oritsi@bgu.ac.il)

Abstract. Dissimilatory iron reduction is probably one of the oldest types of metabolisms that still participates in important biogeochemical cycles, such as the carbon and sulfur cycles. It is one of the more energetically favorable anaerobic microbial respiration processes and is usually coupled to the oxidation of organic matter. Traditionally this process is thought to be limited to the shallow part of the sedimentary column in most aquatic systems. However, iron reduction has also been observed in the methanic zone of many marine and freshwater sediments, well below its expected zone, occasionally accompanied by decreases in methane, suggesting a link between the iron and the methane cycles. Nevertheless, the mechanistic nature of this link (competition, redox or other) has yet to be established, and has not been studied in oligotrophic shallow marine sediments. In this study we present combined geochemical and molecular evidences for microbial iron reduction in the methanic zone of the oligotrophic Southern Eastern (SE) Mediterranean continental shelf. Geochemical pore-water profiles indicate iron reduction in two zones, the uppermost part of the sediment, and the deeper zone, located in the enhanced methane concentration layer. Results from a slurry incubation experiment indicate that the deep methanic iron reduction is microbially mediated. The sedimentary profiles of microbial abundance and qPCR of the *mcrA* gene, together with Spearman correlation between the microbial data and Fe(II) concentrations in the pore-water, suggest types of potential microorganisms that may be involved in the iron reduction via several potential pathways: H_2 or organic matter oxidation, an active sulfur cycle or iron driven anaerobic oxidation of methane. We suggest that intensive upward migration of methane in the sedimentary column and its oxidation by sulfate may fuel the microbial activity in the sulfate methane transition zone (SMTZ). The biomass, created by this microbial activity, can be used below by the iron reducers in the methanic zone of the sediments of the SE Mediterranean.

1 Introduction

Iron (Fe) is the fourth most abundant element in the Earth's crust. It appears as elemental Fe, Fe(II) and Fe(III), and has an important geobiological role in natural systems (e.g. Roden, 2006). Dissimilatory microbial iron reduction may be one of the first evolutionary metabolisms, and plays a key role in the reductive dissolution of Fe(III) minerals in the natural environment (Lovley and Phillips, 1986; Lovley

et al., 1987; Lovley and Phillips, 1988; Lovley, 1997; Weber et al., 2006) and in the mineralization of organic matter in freshwater sediments (Roden and Wetzel, 2002). It also serves as a redox wheel that drives the biogeochemical cycles of carbon, nitrogen, sulfur and phosphorous (Li et al., 2012 ; Slomp et al., 2013; Sivan et al., 2014; Egger et al., 2016; Ettwig et al., 2016; Riedinger et al., 2017; März et al., 2018).

Dissimilatory iron reduction is part of the anaerobic respiration cascade, in which different organic substrates are used for energy by microorganisms and oxidized to dissolved inorganic carbon (DIC). This is accomplished by reduction of electron acceptors, other than oxygen, according to their availability and energy yield. Denitrification is the first respiratory process in anoxic sediments, followed by manganese reduction, iron reduction and then sulfate reduction. Methane (CH_4) production (methanogenesis) by archaeal methanogens is traditionally considered to be the terminal process of microbial organic matter mineralization in anoxic environments, after the other electron acceptors have been exhausted (Froelich et al., 1979). When the produced methane diffuses away from the methanic layer and meets an electron acceptor it can be consumed by microbial oxidation (methanotrophy). In marine sediments anaerobic oxidation of methane (AOM) coupled to sulfate reduction has been shown to occur (Iversen and Jørgensen, 1985; Hoehler et al., 1994; Hinrichs et al., 1999; Boetius et al., 2000; Orphan et al., 2001; Knittel and Boetius, 2009), and was found to consume up to 90 % of the methane that diffuses upwards to the sulfate methane transition zone (SMTZ) (e.g. Neiwöhner et al., 1998; Valentine, 2002).

The classical process of dissimilatory iron reduction is coupled to the oxidation of organic matter (organoclastic iron reduction) (Eq. 1, Lovley, 1991; Lovley et al., 1996). However, iron reduction can be coupled to other processes as well, such as hydrogen (H_2) oxidation (hydrogenotrophic iron reduction) (Eq. 1, Lovley, 1991). Additionally, Fe(III) can be reduced microbially (and also abiotically) by pyrite oxidation (Eq. 2, Bottrell et al., 2000), leading to sulfur (S) intermediates, and followed by their disproportionation to sulfate and sulfide via a "cryptic" sulfur cycle (e.g. Holmkvist et al., 2011).

$$2Fe^{3+} + organic\ matter/H_2/humic\ acids \rightarrow 2Fe^{2+} + HCO_3^-/CO_2/2H^+ \qquad (1)$$

$$FeS_2 + 14Fe^{3+} + 8H_2O \rightarrow 15Fe^{2+} + 2SO_4^{2-} + 16H^+ \qquad (2)$$
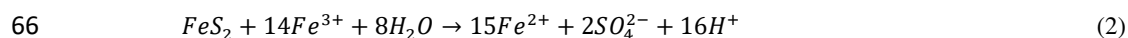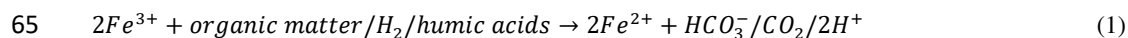
Another recently discovered pathway of iron reduction is by AOM (Eq. 3).

$$CH_4 + 8Fe(OH)_3 + 15H^+ \rightarrow HCO_3^- + 8Fe^{2+} + 21H_2O \qquad (3)$$
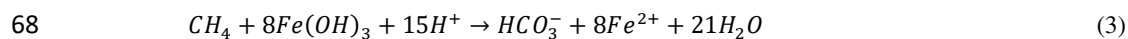
This process in marine sediments was shown through incubation experiments with marine seeps sediments (Beal et al., 2009; Sivan et al., 2014). It was also suggested to exist mainly through geochemical profiles in deep sea sediments and their modeling (Sivan et al., 2007; März et al., 2008; Riedinger et al., 2014), and in brackish coastal sediments (Slomp et al., 2013; Segarra et al., 2013; Egger et al., 2014; Egger et al., 2016; Rooze et al., 2016; Egger et al., 2017). In freshwater environments, it was suggested to occur in lakes (Crowe et al. 2011; Sivan et al., 2011; Norði et al., 2013), and in denitrifying cultures from sewage, where it was performed by methanogens (Ettwig et al., 2016). Iron-coupled AOM in natural lake sediments was indicated using isotope pore-water depth profiles (Sivan et al., 2011), rate modeling based on these profiles (Adler et al., 2011), microbial profiles (Bar-Or et al.,

78   2015), and directly from a set of sediment slurry incubation experiments (Bar-Or et al. 2017). The few
79   microbial studies on iron-coupled AOM (mainly in cultures) showed either the involvement of
80   methanogenic/methanotrophic archaea (Scheller et al., 2016; Ettwig et al., 2016; Rotaru and Thamdrup,
81   2016; Cai et al., 2018; Yan et al., 2018) or a cooperation between methanotrophs and methanogens (Bar-
82   Or et al., 2017).

83   Whereas Fe(II) is highly soluble, Fe(III) which is the most abundant species of iron under natural
84   conditions, appears as low-solubility oxidized minerals. This makes iron usage a challenge to
85   microorganisms, which need to respire these iron-oxide minerals, thus rendering many of the iron-oxide
86   minerals effectively unavailable for reduction and leading to the dominance of sulfate reducing bacteria
87   beyond a certain depth. Therefore, it is not trivial to observe iron reduction below the upper iron reduction
88   depth, in the methanic zone, where iron-oxides are assumed to be of low reactivity. Moreover, this type
89   of iron reduction is occasionally accompanied by depletion in methane concentrations, suggesting a
90   possible link between the iron and the methane cycles. There are three potential mechanisms that can
91   link the cycles: 1) a competition between methanogens and iron-reducing bacteria over substrate, 2) a
92   metabolism switch of methanogens from methanogenesis to iron reduction, and 3) iron coupled AOM,
93   as mentioned above. Previous observations in other environments demonstrated the inhibition of
94   methanogenesis under iron-reducing conditions due to competition between methanogens and iron-
95   reducing bacteria for the common acetate and hydrogen substrates (Lovley and Phillips, 1986; Roden
96   and Wetzel, 1996; Conrad, 1999; Roden, 2003). Different methanogens can also utilize iron directly, by
97   reducing Fe(III). This was shown in pure cultures with the amorphous Fe(III) oxyhydroxide (Bond and
98   Lovley., 2002), in pure cultures close to natural sedimentary conditions (Sivan et al., 2016), in natural
99   lake sediments with different iron oxides (i.e. amorphous iron, goethite, hematite and magnetite) (Bar-or
100   et al., 2017), in anoxic ferruginous lake sediment enrichments (Bray et al., 2018), and in iron-rich clays
101   (Liu et al., 2011; Zhang et al., 2012; Zhang et al., 2013).

102   Despite the above studies, the nature of the link between the biogeochemical cycles of iron and methane
103   in the methanic zone of marine sediments, which creates suitable conditions for iron reduction, has not
104   yet been determined. Furthermore, this microbial iron reduction in methanic zones has not been shown
105   in the sediments of oligotrophic shallow marine environments. In this study we report the observation of
106   microbial iron reduction in the methanic depth of marine sediments from the oligotrophic SE
107   Mediterranean continental shelf. The microbial iron reduction is observed by using geochemical pore-
108   water profiles, qPCR profile of archaea, bacteria and the *mcrA* functional gene and 16S rRNA gene
109   sequencing profile at three different stations combined with a simple slurry incubation experiment from
110   the methanic zone. The slurries were amended with hematite and magnetite. Given their low reactivity
111   these are the expected Fe(III) minerals to survive the sulfide zone (Canfield, 1989; Poulton et al., 2004).
112   Furthermore, these minerals were found to be active in iron-coupled AOM in lake sediments (Bar-Or et
113   al., 2017). The profiles, the incubation experiment as well as the related microorganisms, are discussed
114   in terms of the possible links between the cycles of iron and methane.

2 Methods

2.1 Study site

The surface water in the Levantine Basin of the SE Mediterranean Sea, including Israel's continental shelf, is an oligotrophic nutrient-poor marine system (Herut et al., 2000; Kress and Herut, 2001). The continental shelf narrows from south to north and is composed of Pliocene-Quaternary Nile-derived sediments. The sedimentation rate decreases with increasing distance from the Nile Delta and from the shoreline (Nir, 1984; Sandler and Herut, 2000). Off the shore of Israel, the sedimentation rate is relatively high at ~0.1 cm y^{-1} (Bareket et al., 2016). The bottom seawater along the continental shelf is well oxygenated and sulfate concentrations at the water-sediment interface are ~30 mmol L^{-1} (Sela-Adler et al., 2015). The central and eastern regions of the Levantine Basin have relatively low total organic carbon (TOC) content (~0.1 – 1.4%; Almogi-Labin et al., 2009; Sela-Adler et al., 2015; Astrahan et al., 2017) as compared to the Western Mediterranean Basin and offshore the Nile River delta (1 – 2%). Along the Egyptian coast, the TOC in surface sediments on the shelf reach maximum values of 1.5% (Aly Salem et al., 2013). The finding of a free gas zone, which is located from few to tens meters below the seafloor (i.e. gas front), in seismic profiles within the sediments of the continental shelf of Israel (Schattner et al., 2012) led to the discovery of biogenic methane formation at some locations in the shallow sediments (Sela-Adler et al., 2015).

2.2 Sampling

Seven sediment cores (~5 – 6 m long) were collected using a Benthos 2175 piston corer, from the undisturbed sediments of the SE Mediterranean continental shelf of Israel at water depths of 81 – 89 m from three stations; SG-1, PC-3 and PC-5 (Fig. 1). The cores were sampled during cruises of R.V. *Shikmona* between 2013 to 2017, and by the R.V. *Bat-Galim* on January 2017 (Table 1). The sediment cores were sliced on board every 25 – 35 cm within minutes upon retrieval from the seafloor. This area was previously investigated for other purposes, such as the sulfate reduction in the SMTZ (Antler et al., 2015; Wurgaft et al., 2019.), and the possibility of methanogenesis (Sela-Adler et al., 2015).

From each interval, a 2.5 mL of sediment sample was collected and inserted immediately into an anoxic 10 mL glass bottle filled with 5 mL NaOH 1.5 N for headspace measurements of methane concentration (after Nüsslein et al, 2003). Approximately 3 mL of sediment was sampled every 50 cm for porosity. In addition, another 2.5 mL sediment sample was taken from each segment of the cores and transferred into a 20 mL glass bottle filled with NaCl saturated solution for H$_2$ concentrations measurements. Sediment samples from each segment of the cores were centrifuged on board if possible or in the lab within a day by Sorval centrifuge at 9500 RPM under 4 °C and Ar atmosphere in order to extract pore-water for chemical analysis. The supernatant was filtered (0.22 µm) and analyzed for Fe(II), sulfate, sulfide, DIC and the stable carbon isotope composition of the DIC ($\delta^{13}C_{DIC}$). After the pore-water extraction, the sediment was analyzed for the content of the different reactive iron minerals (Table 2). In addition, sediment sub-sample from each segment of the January 2017 core from Station SG-1 was kept at -20 °C for molecular analysis. Due to high water content and movement in the uppermost part of the sediments, two ~30 cm sediment cores were also sub-sampled separately, using a 0.0625 m^2 box corer (Ocean

153   Instruments BX 700 Al) and Perspex tubes during the September 2015 and January 2017 cruises. The

154   short cores were stored at 4 °C, cut in the lab within 24 hours after their collection and their results are

155   presented for the top sediment (Fig. 2a – d).

2.3 Slurry incubation experiment

157   The experimental set-up (Table 2) consisted of 11 bottles with sediment from the methanic zone (265-

158   285 cm depth) from Station SG-1, where iron reduction was apparent from the pore-water profiles (Fig.

159   2d). Prior to the beginning of the experiment, sediment from the designated depth had been homogenized

160   in an anoxic bag under N_2 atmosphere. It was then transferred under anoxic conditions to a 250 mL glass

161   bottle with the addition of synthetic sea water without sulfate to reach a 1:1 sediment:water slurry ratio

162   for 3 months incubation period. After the incubation period the slurry was sub-divided anoxically to the

163   11 experiment bottles (60 mL each), and synthetic sea water was added for final sediment:water ratio of

164   1:3. The bottles were sealed with a crimped cap and were flushed with N_2 for 5 minutes, shaken

165   vigorously and flushed again, (repeated 3 times). Three experimental bottles were autoclaved twice to

166   serve as "killed" control for the experiment. The experimental bottles were amended with 1.6 g L^{-1} of

167   hematite (Fe_2O_3) or 2.3 g L^{-1} of magnetite (Fe_3O_4) to reach Fe(III) final concentration of 10 mmol L^{-1}.

168   The three killed bottles were amended with the iron oxides after they cooled down to room temperature.

169   H_2 was added to some treatments to test its potential as an electron donor. One mL of H_2 was injected by

170   gas tight syringe to the three killed bottles, to two bottles with the addition of hematite and to two bottles

171   with the addition of magnetite (to reach final concentration of ~4% of the head space volume). The

172   experimental bottles were sampled several times for dissolved Fe(II) concentrations during the 14 day

173   experiment period.

2.4 Analytical methods

2.4.1 Pore-water analyses

176   Methane concentrations in the pore-water were analyzed by Focus Gas Chromatograph (GC; Thermo)

177   equipped with FID detector with a detection limit of 50 µmol L^{-1}. To calculate the methane concentrations

178   the sediment porosity was considered. Porosity was determined by drying wet sediment samples at 60

179   °C until there was no weight loss (~48 h). It was calculated as the weight loss from the initial weight of

180   the samples. H_2 concentrations were analyzed in a Reducing Compound Photometer Gas Chromatograph

181   (RCP-GC; Peak Laboratories). Dissolved Fe(II) concentrations were measured using the ferrozine

182   method (Stookey, 1970) by a spectrophotometer at 562 nm wavelength with detection limit of 1 µmol L^{-}

183   ^{1}. Sulfide was measured using the Cline (1969) method by a spectrophotometer at 665 nm wavelength

184   with detection limit of 1 µmol L^{-1}. Total sulfur concentrations were measured in an inductively coupled

185   plasma atomic emission spectrometer (ICP-AES), Perkin Elmer Optima 3300, with an analytical error of

186   ±1% (average deviations from repeated measurements of a seawater standard). Since sulfide was not

187   detected in any of the sediment cores, the total sulfur concentration in each pore-water sample was

188   assumed to be the sulfate concentration of that sample. The $\delta^{13}C_{DIC}$ values were measured on a DeltaV

189   Advantage Thermo© isotope-ratio mass-spectrometer (IRMS) at a precision of ±0.1 ‰. Results are

190   reported versus VPDB standard. Pore-water profiles of dissolved total sulfur, CH_4, $\delta^{13}C_{DIC}$, Fe(II) and

191   H_2 were produced during the study, and all of them are presented (Fig. 2). For each profile where

192   duplicate samples were taken the error bar is that of the average deviation of the mean of the duplicates,

193   in cases where only single samples were taken, it is the analytical error (if larger than the symbol).

2.4.2 Sediment analysis

195   Reactive Fe(III) in the sediments was measured according to Poulton and Canfield (2005) definition and

196   sequential extraction procedure. The different reactive iron minerals were separated to (1) carbonate-

197   associated Fe (Fe_{carb}) (i.e. siderite and ankerite); (2) easily reducible oxides (Fe_{ox1}) (i.e. ferrihydrite and

198   lepidocrocite); (3) reducible oxides (Fe_{ox2}) (i.e. hematite, goethite and akageneite) and (4) magnetite

199   (Fe_{mag}). Sediment samples were dried at 60°C, then, approximately 0.6 g dry sediment was inserted to a

200   centrifuge tube with 10 ml of a specific extractant at every stage under atmospheric conditions and

201   constant agitation (Table 3). The fluids were separated from the sediment by centrifugation and removed

202   from the tube with Pasteur pipette after every extraction stage. At the end of each extraction stage, the

203   extractant was transferred to a 15 mL falcon tube with 0.1 mL ascorbic acid and 0.1 mL ferrozine solution

204   to reduce all the Fe(III) to Fe(II) and fix it, then it was measured spectrophotometrically. The results

205   presented as "total reactive Fe(III)" are the sum of Fe_{ox1}, Fe_{ox2} and Fe_{mag}. The profile of pyrite (Fe_{py}) was

206   taken from Wurgaft et al., (2019).

2.4.3 Quantitative PCR and 16S rRNA gene V4 amplicon pyrosequencing

208   DNA was extracted from the sediment core of Station SG-1 from January 2017 using Power Soil DNA

209   Kit (MoBio Laboratories, Inc., Carlsbad, CA, USA) following manufacturer's instructions. Copy

210   numbers of selected genes were estimated with quantitative PCR (qPCR) as described previously (Niu

211   et al., 2017) using specific primers: Uni519f/Arc908R and bac341f/519r for archaeal and bacterial 16S

212   rRNA genes, respectively, and mlas/mcrA-rev for the *mcrA* gene, which encodes the α-subunit of methyl-

213   coenzyme M reductase. The amplification efficiency was 94.5%, 106.3% and 92.4% for the archaeal 16S

214   rRNA, bacterial 16S rRNA and the *mcrA* gene, respectively (the respective R^2 of the standard curve was

215   0.998, 0.998 and 0.995).

216   The V4 regions of bacterial and archaeal 16S rRNA genes were amplified using barcoded 515FB/806RB

217   primers (Walters et al., 2015) and Arch519/Arch806 primers (Song et al., 2013), respectively. PCR

218   mixture contained 6 – 10 ng total DNA, 5 μL 10× Ex Taq buffer, 4 μL 2.5 mmol L^{-1} dNTP mix, 1 μL of

219   each primer, 0.25 μL Ex Taq polymerase (Ex-Taq; TaKaRa, Dalian, China) and 5 μL bovine serum

220   albumin (25 mg mL^{-1}) in a total volume of 50 μL. DNA was sequenced as 2x150 bp reads using Illumina

221   MiSeq platform (Illumina, USA). Sequence quality assessments, chimera detection and down-stream

222   phylogenetic analyses were conducted in QIIME (Caporaso et al., 2010). Taxonomic assignments for

223   each OTU were performed in QIIME using the BLAST method and the SILVA128 reference database.

224   24056 to 132042 high quality sequences were obtained per sample, with the proportion of high-quality

225   sequence versus total sequence between 81.97 – 99.89%. Spearman correlation was performed using the

226   online calculator (http://www.sthda.com/english/rsthda/correlation.php) to test the relevance of

227   microbial abundance and communities with Fe(II) concentration along the depth of the sediment core

228   from 185 cm to the bottom 575 cm, which is the methanic zone of the sediment core according to the

229   geochemical profile (see the results below).

 3 Results

231 **3.1 Geochemical profiles**

232 Geochemical pore-water profiles of several sediment cores from the three stations (SG-1, PC-3 and PC-

233 5 (Fig. 1, Table 1)) were produced in order to characterize the iron reduction process in the methanic

234 zone of the SE Mediterranean continental shelf and to identify its potential sources. The pore-water

235 profiles at Station SG-1 (Fig. 2a) show complete depletion of total sulfur at approximately 150 cm depth

236 in all cores. Sulfide concentrations were below the detection limit in all cores, indicating that the total

237 sulfur is mostly sulfate. The methane concentrations in the pore-water (Fig. 2b) show an increase with

238 depth immediately after the consumption of sulfate. The maximum methane concentration was

239 approximately 10 mmol L^{-1} at ~140 cm depth in June 2015. The other methane depth profiles show an

240 increase in the concentrations to approximately 2 mmol L^{-1} and then leveling off throughout the bottom

241 of the cores (~600 cm). Detected dissolved Fe(II) concentrations (Fig. 2d) were found in the upper iron

242 reduction zone (between 30 – 90 cm depth), and a second peak was found in the deeper part of the

243 sediment, at the methanic zone (below 180 cm depth). Maximum dissolved Fe(II) concentrations reached

244 84 µmol L^{-1} in the upper iron reduction zone of the sediments and 65 µmol L^{-1} in the methanic zone. The

245 $\delta^{13}C_{DIC}$ values (Fig. 2c) were the lowest (-35 ‰) as expected at the SMTZ depth, and the highest in the

246 methanic zone. H_2 concentrations (Fig. 2e) decreased to a minimum of 0.017 µmol L^{-1} at 155 cm depth,

247 and then increased to a maximum of 0.147 µmol L^{-1} at 485 cm depth.

248 Pore-water profiles from Station PC-3 (Fig. 2g – l) show similar patterns to Station SG-1 on all three

249 sampling dates, but with lower methane concentrations. Total sulfur (Fig. 2g) was completely depleted

250 within the upper 300 cm depth. Sulfide concentrations were below the detection limit at this station as

251 well. Methane profiles show an increase in methane concentration immediately after the consumption of

252 sulfate. The maximum methane concentration (Fig. 2h) reached 0.8 mmol L^{-1} at 450 cm depth in the

253 Aug-13 core. The dissolved Fe(II) profiles (Fig. 2j) show two peaks at this station as well, one in the

254 upper part of the sediment with maximum value of 32 µmol L^{-1} at 177 cm depth, and another one with

255 maximum value of 64 µmol L^{-1} at 390 cm depth at the methanic depth. The $\delta^{13}C_{DIC}$ values (Fig. 2i)

256 decreased from approximately -10 ‰ at the water-sediment interface to -20 ‰ at the SMTZ. Below that

257 zone there was an increase in $\delta^{13}C_{DIC}$ values to about -5 ‰ due to methanogenesis. H_2 concentrations

258 (Fig. 2k) remained around 2 µmol L^{-1} along the core. The three deviating points that do not fit the clear

259 pattern are attributed to an analytical or sampling error.

260 Pore-water profiles from the core collected at Station PC-5 (Fig. S1) resemble the profiles of Station PC-

261 3. Total sulfur was depleted at approximately 300 cm, and methane concentrations increased below that

262 depth to 0.3 mmol L^{-1}. The Fe(II) profile shows two peaks in this core as well, one in the upper sediment

263 of 20 µM at 150 cm depth and the second of 30 µmol L^{-1} in the methanic zone. The $\delta^{13}C_{DIC}$ value

264 decreased from -5 ‰ at the water-sediment interface to -25 ‰ at the SMTZ, and below that depth

265 increased to -17 ‰ at the methanic zone.

266 In addition to the dissolved constituents' profiles, reactive iron minerals were extracted from the sediment

267 collected on September 2015, and operationally defined iron mineral fractions profiles from Stations SG-

268 1 and PC-3 were produced (Fig. 2f and l). In Station SG-1 there appears to be a slight variability in the

269 content of the minerals (Fig. 2f). The Fe_{carb} content in the upper part of the sediment was 0.22 dry wt%,

270 increased to ~0.45 dry wt % at 103 cm depth and then remained constant. The Fe_{ox1} content was 0.49 dry

271 wt % in the upper part of the sediment, peaked at 203 cm depth to 0.64 dry wt % and then decreased to

272 0.50 dry wt % at the bottom of the core. The Fe_{ox2} content was 2.15 dry wt % in the upper part of the

273 sediment, decreased to 1.03 dry wt % at 312 cm depth, and then it increased to 1.55 dry wt % at 427 cm

274 depth. Fe_{mag} content was 0.34 dry wt % in the upper part of the sediment, decreased to 0.32 dry wt % at

275 153 cm depth, increased to 0.35 at 253 cm depth, decreased to 0.23 dry wt % at 312 cm depth, and

276 increased again to 0.35 dry wt % at the bottom. A pyrite content profile from Station SG-1 was also

277 produced (Wurgaft et al., 2019) from the September 2015 cruise and shows two peaks; the uppermost of

278 1.10 wt % at 153 cm depth, and the lower one of 1.80 wt % at 312 cm depth. The total reactive Fe(III)

279 oxides profile showed a general decrease from 3.00 dry wt % at 13 cm depth to 2.27 dry wt % at 507 cm

280 depth, with two minimum peaks of 2.42 dry wt % at 103 cm and of 1.88 dry wt % at 312 cm.

281 In Station PC-3 there appeared to be smaller changes in the different iron mineral fractions with depth

282 (Fig. 2l). The Fe_{carb} content in the upper part of the sediment was 0.50 dry wt % and reached 0.69 dry wt

283 % in the deep sediment. The Fe_{ox1} content was approximately 1.00 dry wt % throughout the sediment

284 column. The Fe_{ox2} content was 0.78 dry wt % in the upper part of the sediment, increased to 0.89 dry wt

285 % at 167 cm depth and then decreased to 0.76 dry wt % at 495 cm depth. Fe_{mag} content was 0.83 dry wt

286 % in the upper part of the sediment, increased to 0.89 dry wt % at 167 cm, and then decreased again to

287 0.75 dry wt % at 495 cm depth. The total reactive Fe(III) oxides content varied between 2.10 dry wt %

288 (at 167 cm depth) and 1.76 dry wt % (at 137 cm depth).

289 **3.2 Abundance and diversity of bacteria and archaea**

290 The qPCR of bacterial and archaeal 16S rRNA genes from the SG-1 core (collected on January 2017)

291 revealed an abundance of bacterial genes between $1.46 – 9.45 \times 10^6$ copies per g wet sediment, while that

292 of archaea was between $8.15 \times 10^5 – 2.25 \times 10^7$ copies per g wet sediment (Fig. 3). The abundance of

293 bacteria and archaea decreased gradually in the top 95 cm, increased sharply at 125 cm depth within the

294 SMTZ, remained relatively stable with high abundance at 185 – 245 cm (the top layer of the methanic

295 zone), and then decreased. Notably, the abundance of both bacteria and archaea peaked within the

296 methanic zone at 245 cm in correspondence with Fe(II) concentration peak. However, it is not feasible

297 to compare the abundance of archaea and bacteria by this method due to bias caused by the PCR primers

298 used (Buongiorno et al., 2017). The abundance of the *mcrA* gene (Fig. 3) increased sharply from the

299 surface layer to the SMTZ, peaked at 155 cm and remained stable at 155 – 245 cm, indicative of active

300 anaerobic methane metabolism in the SMTZ and an active methanic zone. Spearman correlation test

301 (Table S2) shows that the abundance of the bacteria and archaea 16S rRNA genes and *mcrA* genes

302 correlated with Fe(II) concentration in the methanic zone, where *mcrA* gene correlated the most

303 significantly (r = 0.5429, p value = 0.04789).

304 Illumina-sequencing of the 16S rRNA gene revealed diverse bacterial and archaeal communities

305 throughout the SG-1 core (Fig. 4). Although no clear plateau was observed on species rarefaction curve

306 for the current sequencing depth (Fig. S2), Shannon diversity indices reached stable values, indicating
307 that those sequences well covered the diversity of bacterial and archaeal populations in the samples (Fig.
308 S3). Shannon index, based on 16S rRNA gene sequences, shows higher diversity in the top layers of the
309 sediment along with similar values through the core using the bacterial primers, while for sequences
310 using archaeal primers, the values varied in different layers (Table S1). The bacterial sequences were
311 affiliated with the following phyla: Planctomycetes (25.7%), Chloroflexi (23.2 %), Proteobacteria
312 (12.9%), Deinococcus-Thermus (9.9 %), Acidobacteria (3.5%), Aminicenantes (3.3 %), Spirochaetes
313 (2.3%), Deferribacteres (1.7%), Elusimicrobia (1.6%), Aerophobetes (1.6%), Nitrospirae (1.4%),
314 Firmicutes (1.4 %), Actinobacteria (1.4 %), TM6 (Dependentiae) (1.2%), Marinimicrobia (SAR406 clade)
315 (1.0%), and other taxa with less than 1% of the bacterial communities (Fig. 4a). Bathyarchaeota were the
316 predominant archaea in all the sediment layers, based on the high relative abundance of their 16S rRNA
317 gene sequences (91.0%). The remaining archaeal phyla comprised Euryarchaeota (3.2%),
318 Thaumarchaeota (2.4%), Lokiarchaeota (1.0%), and other phyla with less than 1% of the archaeal
319 communities (Fig. 4b). Spearman correlation analysis (Table S2) revealed that uncultured SBR1093 (r =
320 0.6176, p value = 0.01859) from bacterial Candidate Phylum SBR1093, subgroup 26 of Acidobacteria (r
321 = 0.5841, p value = 0.02828), the uncultured bacterium from TK10 Class of Chloroflexi phylum (r =
322 0.5297, p value = 0.0544) and uncultured Bathyarchaeota sp. (archaea) (r = 0.5516, p value = 0.04388)
323 correlated significantly with Fe(II) concentration.

324 **3.3 Incubation experiment**

325 Sediment from the observed deep iron reduction zone of Station SG-1 from January 2017 core was used
326 for a simple short-term (couple of weeks) slurry incubation experiment in order to characterize the iron
327 reduction process in the methanic zone. Hematite and magnetite, which were expected to survive the
328 sulfate zone, and were shown to be a source for AOM in lake sediments, were added to the slurries.
329 Indeed, the operationally defined iron mineral fractions profiles (Fig. 2f) confirm that hematite and
330 magnetite were abundant in the methanic zone in this core.

331 The results of the experiment are shown in figure 5. Dissolved Fe(II) concentrations show significant
332 increase from 11 μmol L^{-1} to approximately 90 μmol L^{-1} during the first three days in all the experimental
333 bottles, except for the killed bottles, implying that the reduction is microbially mediated. Another
334 observation was that the microorganisms were able to reduce both hematite and magnetite to the same
335 extent. In addition, no difference in the Fe(II) concentrations between bottles with and without the
336 addition of H$_2$ was observed.

337 **4 Discussion**

338 **4.1 General**

339 This study was performed in the SE Mediterranean (Fig. 1) above the area of a recently discovered gas
340 front (Schattner et al., 2012). The investigated methane was found in the shallow sediments (~1-5 m
341 deep) and seems biogenic based on its low $\delta^{13}C_{CH4}$-values and high C1/C2 ratio (Sela-Adler et al., 2015).
342 Station SG-1 is located at the center of the gas front area, while Stations PC-3 and PC-5 are located at
343 the edges, and indeed methane related processes were more intensive at Station SG-1. The source of this

gas front is not certain, but it was speculated to be terrestrial organic matter (Schattner et al., 2012). Our results suggest that there are two sources for methane in our shallow sediment: the first is from migration of methane from this gas front area (Wurgaft et al., 2019), and the second is from *in-situ* methane formation, where the relative contribution of each source is currently unknown. *In-situ* methanogenesis in the shallow shelf sediments is evident by the geochemical profiles of $\delta^{13}C_{DIC}$ and $\delta^{13}C_{CH4}$ (Sela-Adler et al., 2015), by the microbial population abundance profile and by the functional *mcrA* gene profile (Figs. 3 and 4, further discussed below). The TOC content in the methanic zone are ~0.8% at Station SG-1 (Sela-Adler et al., 2015; Wurgaft et al., 2019) and ~1% at Station PC-3 (Sela-Adler et al., 2015), and these levels are known to be able to support *in-situ* methanogenesis (Sivan et al., 2007).

The comparison between the sites show that methane reaches the highest concentrations at Station SG-1 (up to the saturation level (Sela-Adler et al., 2015)), specifically in the June 2015 profile (Fig. 2b). This leads to intensive AOM by sulfate at the SMTZ, causing it to occur at shallower depth and to produce lower $\delta^{13}C_{DIC}$ values than the other two stations. The relation between the upward fluxes of methane, the SMTZ depth and the $\delta^{13}C_{DIC}$ values fit previous studies (e.g. Sivan et al., 2007). The higher methane concentrations in the June 2015 profile is presumably due to intensive migration of methane from the deeper sediments and/or more intensive methane production at the exact location of the core collected at that time. The H_2 concentrations at Station SG-1 (Fig. 2e) were lower by two orders of magnitude than the concentrations at Station PC-3 (Fig. 2k), perhaps due to more intensive hydrogen consuming processes at Station SG-1 (i.e. sulfate reduction, methanogenesis, iron reduction (Conrad et al., 1986; Lovley, 1991). Dissolved Fe(II) pore-water profiles (Figs. 2d and j) show some variability between the cores within the same station, probably as a result of environmental variations.

Despite the pore-water profiles variability between the stations, they show a resemblance in their trends. All geochemical pore-water and iron mineral fraction profiles suggest that the sediments in this area of the SE Mediterranean shelf can be classified into three general depth-zones (Fig. 2): **zone 1** is the upper part of the sediment, where the classical iron reduction occurs, probably coupled to organic matter oxidation, with sulfate reduction below it; **zone 2** is the SMT depth, where methane starts to increase, sulfate is completely depleted, and Fe(II) (Fig. 2d and j) is either present in low concentrations or absent (probably due to the precipitation of iron-sulfide minerals). In addition, the $\delta^{13}C_{DIC}$ values are the lowest in this zone, as expected from the intensive AOM process there, which uses the isotopically light carbon of the methane as a carbon source with small fractionation (Whiticar, 1999; Holler et al., 2009)**; zone 3** is the methanic zone, where methane concentrations increased to the highest values in all stations, as did the $\delta^{13}C_{DIC}$ since the carbon source for the methane comes mainly from CO_2, leaving the residual DIC heavier by about 60 ‰ (Whiticar, 1999; Conrad, 2005). At this zone, local maxima of Fe(II) concentrations in the pore-water were found in all cores, indicating reduction of iron oxides. The slurry experiment results show only a slight increase in Fe(II) concentrations in the killed bottles compared to their significant increase in the non-killed bottles, inferring that the iron reduction in zone 3 is microbial (Fig. 5).

4.2 Potential methanic iron reduction pathways

This observed intensive iron reduction in the methanic sediments is the first discovered in the SE Mediterranean shelf. The phenomenon of iron reduction in the methanic depth has been observed before in other marine provinces (Jørgensen et al., 2004; März et al., 2008; Slomp et al., 2013; Riedinger et al., 2014; Treude et al., 2014; Oni et al., 2015; Egger et al., 2016). Yet, the type of link to the methane cycle is not well understood. Usually, iron reduction is coupled to oxidation of organic matter (Lovley and Phillips, 1988) and is performed by iron-reducing bacteria, which is probably the case in zone 1. It is however questionable if this also stands for zone 3 and if not, what process is responsible for the iron reduction at this depth and its relation to methane. The iron reduction in zone 3 can occur potentially via four pathways: 1) oxidation of organic matter arriving from the SMTZ, where it is produced by the microorganisms that live there and benefit from the upward migrating methane, 2) oxidation of the methane itself, 3) H_2 oxidation or 4) oxidation of sulfur species through a cryptic cycle.

The oligotrophic nature of the water column in the studied area would suggest that intensive bacterial iron reduction coupled with the oxidation of organic matter in zone 3 is less likely. Nevertheless, we observe high methane concentrations in zone 3 in all three stations, where part of it is from upward migration. This indicates that regardless of the surface water oligotrophic nature, the TOC substrate may be enough to sustain all the microbial activity and to take part in the iron reduction process in the methanic zone. This is possibly due to biomass production in the SMTZ (i.e. the microbial community including ANMEs and sulfate reducing bacteria (Boetius et al., 2000)) and its rapid use in the methanic zone (so the TOC content still seems low).

The importance of the methane flux as a carbon source that supports the deep microbial community at zone 2 and 3 in the sediments of the SE Mediterranean can be illustrated by comparing the organic carbon flux from the photic zone, with the flux of organic carbon that is oxidized by sulfate in the pore-water. Using traps, Moutin and Raimbault (2002) estimated an export flux of 7.4±6.3 mgC m^{-2} d^{-1}, which leaves the photic zone. However, Wurgaft et al. (2019) estimated that the flux of DIC toward the SMTZ from sulfate reduction is equivalent to 8±3 mgC m^{-2} d^{-1}. Whereas the difference between the two fluxes is statistically insignificant, it should be noted that the flux of organic material that survives aerobic oxidation in the water column and the upper part of the sediment column, as well as anaerobic oxidation by other electron acceptors with higher energy yield (Froelich et al., 1979; Emerson et al., 1980), is likely to be substantially smaller than the flux measured by Moutin and Raimbault (2002). Therefore, it is unlikely that export flux from the photic zone constitutes the sole source of carbon to the SMTZ. Wurgaft et al. (2019) suggested that "external" methane, originates in deeper portions of the sediments, provides an important source of carbon to the SMTZ in Station SG-1. Such fluxes of "external" methane are common along continental margin sediments (e.g. Milkov and Sassen, 2002; Milkov, 2004; Zhang and Lanoil, 2004; Paull et al., 2008; Fischer et al., 2013). Here, we suggest that this supply of methane, leads to intensive sulfate-mediated AOM in the SMTZ, and that this intensive process and biomass may serve as an additional substrate that "fuels" zone 3, activating the iron-oxides.

The recently discovered iron-coupled AOM process (Eq. 3) is the second potential process that can involve iron-oxide reduction in the deep methanic zone (Sivan et al., 2011: Segarra et al., 2013; Slomp

420 et al., 2013; Riedinger et al., 2014; Egger et al., 2015; Rooze et al., 2016; Egger et al., 2017; Bar-Or et
421 al., 2017). Fe(III) as an electron acceptor for AOM provides a greater free energy yield than sulfate
422 (Zehnder and Brock, 1980), and its global importance was emphasized (Sivan et al., 2011: Segarra et al.,
423 2013; Sivan et al., 2014). Two of the main environmental conditions for iron-coupled AOM to occur are
424 high dissolved methane concentrations and abundant reducible iron oxides (Riedinger et al., 2005;
425 Riedinger et al., 2014; Egger et al., 2017). Thus, from our profiles it seems that AOM could be a valid
426 option, considering the high methane concentrations and the high sedimentation rates (0.1 cm y^{-1} (Bareket
427 et al., 2016)), which allow the iron oxides to survive the sulfidic zone and reach the methanic zone
428 (Riedinger et al., 2005; Riedinger et al., 2014; Egger et al., 2017). This can also be inferred from figure
429 6, where some association was observed between the dissolved Fe(II) concentrations and the methane
430 concentrations in zone 3. It seems that at high concentrations of Fe(II), methane concentrations are low
431 and vice versa. This could be a result of iron-coupled AOM that uses methane to reduce Fe(III)-oxides,
432 releasing dissolved Fe(II) to the pore-water. It can also suggest a type of competitive relationship between
433 methanogenesis and microbial iron reduction, or microbial population switching from methanogenesis
434 to iron reduction metabolism (e.g. Sivan et al., 2016). It should be noted that our experiment was not
435 designed to test AOM due to its short time scale of a few weeks, hence another long experiment with the
436 addition of the ^{13}C-labeled methane will enable us to shed more light on this association.

437 The third potential process that can be coupled to iron reduction in the methanic zone is H_2 oxidation. H_2
438 is an important intermediate in anoxic aquatic sediments. In this type of environment, it is produced
439 mainly by fermentation of organic matter (Chen et al., 2006), and can be involved in different microbial
440 processes where each process would need a certain amount of H_2 in order to occur (Lovley and Goodwin,
441 1988). The H_2 levels at Stations SG-1 and PC-3 (Fig. 2e and k) are relatively high in comparison to other
442 marine environments (Lilley et al., 1982; Novelli et al., 1987), suggesting that there is enough H_2 to
443 sustain the iron reduction process. The relatively high H_2 concentrations at these stations could be
444 explained by the dominance of H_2 production processes (i.e. fermentation (Chen et al., 2006)) compared
445 to H_2 consuming processes (i.e. sulfate reduction, methanogenesis, iron reduction (Conrad et al., 1986;
446 Lovley, 1991)). At Station PC-3, the H_2 concentrations (Fig. 2k) are constant in zone 3, this suggest that
447 in addition to being produced, H_2 is consumed as well. At Station SG-1 (Fig. 2e) there is a maximum
448 peak at zone 3, indicating that there is either more H_2 production or less H_2 consumption at this zone
449 compared to zone 2. This is reasonable considering the intensive microbial activity in zone 2. The
450 decrease in the H_2 concentrations below the peak suggests that H_2 consuming processes are intensive in
451 this zone. The H_2 involvement was tested by injecting 1 mL of this gas to the experimental bottles in the
452 methanic iron reduction process (Fig. 5). We observed that the increase of Fe(II) concentration was
453 similar in the bottles with H_2 addition compared to the bottles without H_2. This could mean that either
454 there is enough H_2 in the sediments as it is, as implied by the H_2 pore-water profiles, or that at the
455 methanic depth H_2 is not involved in the iron reduction process.

456 The fourth potential way to reduce iron in zone 3 is by an active sulfur cycle. The pyrite profile supports
457 this possibility by showing two peaks, uppermost in zone 2 of ~1 wt% and the other in zone 3 of ~2 wt%
458 at about 300 cm depth (Fig. 2f). The peak at 300 cm depth indicates possible active sulfur cycle, even

though sulfate is already undetected at 200 cm. Thus, a possible scenario is that Fe(III) is reduced by pyrite oxidation (Eq. 3) (Bottrell et al., 2000), which triggers the 'cryptic' sulfur cycle, as observed in other marine sediments (Holmkvist et al., 2011; Brunner et al., 2016; Egger et al., 2016). In this cycle, elemental sulfur, and eventually by disproportionation also sulfide and sulfate, are produced. The sulfide reacts with iron-oxide and precipitates as FeS or as pyrite (FeS_2) (Holmkvist et al., 2011). The sulfate can inhibit methanogenesis (Mountfort et al., 1980; Mountfort and Asher, 1981), which can result in the enhancement of the iron reduction process due to competition for substrate with the methanogenesis process. Another indication for an active sulfur cryptic cycle comes from the 16S rRNA sequencing analysis (Fig. 4), which shows that Proteobacteria, a potential sulfur related bacteria phylum, is one of the most abundant phyla in the sediments. Moreover, the increase in the abundance of Sva0485 order of the deltaproteobacteria class, a known sulfate reducer (Tan et al., 2019), with depth supports an active sulfur cycle in zone 3 as well.

4.3 Potential microbial players

Our data profiles and incubations indicate that the observed iron reduction in the methanic zone of the SE Mediterranean shelf is performed by microbial activity. The microbial results show first that the abundances of the bacteria and archaea (Fig. 4) are typical to oligotrophic marine sediments (e.g. South China Sea that contains ~0.5 – 1 % TOC (Yu et al., 2018)). Second, even though potential bacterial iron reducers, such as *Alicyclobacillus*, *Sulfobacillusin*, *Desulfotomaculum* genera (Firmicutes), *Acidiphilium* (Alphaproteobacteria), *Desulfobulbus*, *Desulfuromonas*, *Geobacter*, *Geothermobacter*, *Anaeromyxobacter* (Deltaproteobacteria) and *Shewanella* (Gammaproteobacteria) (Weber et al., 2006) comprise less than 0.1% of bacteria detected in the methanic zone (from 185 cm and below), it appears that both the microbial abundance and the Fe(II) concentration peaked at this zone. Cultivation efforts indicated that archaeal methanogens may also play a role in iron reduction within sediments (Sivan et al., 2016). Moreover, the relative abundance of methane-metabolizing archaea was shown to correlate with Fe(II) concentrations in Helgoland muds from the North Sea, where microbial abundance and the Fe(II) concentrations peaked at the methanic zone (Oni et al., 2015), similarly to the results found in the SE Mediterranean sediments. It is possible that methane-metabolizing archaea were involved in the iron reduction in the SE Mediterranean sediments, as the highest *mcrA* gene copies per gram wet sediment were detected in the SMTZ and in the top of the methanic zone (Fig. 3) where the Fe(II) concentrations are high (Fig. 2d). Methanotrophs, such as ANMEs, were found to be involved in iron-coupled AOM in marine and freshwater cultures (Scheller et al., 2016; McGlynn et al., 2015; Ettwig et al., 2016; Cai et al., 2018). ANMEs were found here with relatively low frequencies (ANME1, below 1% in most samples, circa 5% in the 185 cm layer), and their role in iron reduction within the SE Mediterranean sediments remains to be tested.

In our study, Spearman correlation analysis at Station SG-1 (Table S2) revealed that bacterial phyla SBR1093 (candidate Phylum), Acidobacteria and Chloroflexi, as well as archaeal Phylum Bathyarchaeota showed significant positive correlation with a Fe(II) concentration in the methanic zone. The Candidate Phylum SBR1093 was firstly identified in phosphate-removing activated sludge from a sequencing batch reactor (Bond et al., 1995), and continuously detected in a short-chain fatty acid rich

environment such as wastewater treatment, and marine sediments (Wang et al., 2014). It was thought to be capable of growing autotrophically, but the metabolic capabilities related to iron reduction remain unclear. Strains of Acidobacteria and Chloroflexi phylum were found to be capable of iron reduction (Kawaichi et al., 2013; Kulichevskaya et al., 2014). In addition, members of Acidobacteria were found in iron-coupled AOM enrichment (Beal et al., 2009). The metabolic properties of Subgroup 26 from Acidobacteria and TK10 Class of Chloroflexi are still not known. Bathyarchaeota are globally distributed and account for a considerable fraction of the archaeal communities in the marine sediments, particularly, in the Mediterranean Pleistocene sapropels (Coolen et al., 2002; Zhou et al., 2018). While Bathyarchaeota have diverse metabolic capabilities (Lloyd et al., 2013; Meng et al., 2014; Evans et al., 2015; He et al., 2016; Yu et al., 2018; Feng et al., 2019), their role in iron reduction warrants further studies, as suggested from their high abundance here. Therefore, iron reduction and methane cycling within the deep methanic zone may be facilitated by an interplay among bacterial and archaeal groups, whose physiology and functions needs further investigation.

5 Conclusions

Our study used combined geochemical and microbial profiles together with a slurry incubation experiment to show microbial iron reduction in methanic sediments, and the potential microbial population performing this reduction. The Spearman analysis points out several potential microbial players (both bacterial and archaeal) that correlate to the dissolved Fe(II) profiles (e.g. Bathyarchaeota, Acidobacteria and Chloroflexi). Moreover, our study emphasizes that this iron reduction in the methanic zone can occur even in sediments of oligotrophic seas such as the SE Mediterranean. We suggest that the availability of iron minerals for reduction is linked to intensive upward fluxes of methane and high sulfate-AOM rates that may produce available biomass or/and hydrogen, which fuel deeper microbial processes. The deep iron reduction may also be linked to a cryptic sulfur cycle and iron-coupled AOM.

5 Author contribution

H.V and O.S designed research; B.H and O.S. were the PIs of the cruises; H.V, E.W and L.L performed research and analyzed the data; H.V, O.S, B.H, F.W, M.RB and L.L synthesized the data and wrote the paper.

The authors declare that they have no conflict of interest.

6 Acknowledgments

We thank the captain and crew of the R/V Shikmona and R/V Bat Galim from the Israel Oceanographic and Limnological Research for all their help during field sampling. Many thanks to E. Eliani-Russak for her technical assistance in the lab and to V. Boyko for her help with the reactive iron speciation procedure. We also thank all of Prof. O. Sivan's lab members for their help. We would like to thank also to the anonymous reviewers for their helpful and constructive comments. This study was supported by the joint grant of Israel Science Foundation and the National Natural Science Foundation of China (ISF-NSFC) [grant number 31661143022 (FW) and 2561/16 (OS)]. Funding was provided to H. Vigderovich by the Mediterranean Sea Research Center of Israel.

535   **References**

536   Adler, M., Eckert, W. and Sivan, O.: Quantifying rates of methanogenesis and methanotrophy in Lake
537   Kinneret sediments (Israel) using pore-water profiles, Limnol. Oceanogr., 56(4), 1525–1535,
538   doi:10.4319/lo.2011.56.4.1525, 2011.

539   Almogi-Labin, A., Herut, B., Sandler, A. and Gelman, F.: Rapid changes along the Israeli
540   Mediterranean coast following the damming of the Nile and their influence on the Israeli inner shelf.
541   Geol. Surv. of Israel, Israel, 32, 2009.

542   Antler, G., Turchyn, A. V, Herut, B. and Sivan, O.: A unique isotopic fingerprint of sulfate-driven
543   anaerobic oxidation of methane, Geology, 43(7), 1–4, doi:10.1130/G36688.1, 2015.

544   Astrahan, P., Silverman, J., Gertner, Y. and Herut, B.: Spatial distribution and sources of organic
545   matter and pollutants in the SE Mediterranean (Levantine basin) deep water sediments, Mar. Pollut.
546   Bull., 116(1–2), 521–527, doi:10.1016/j.marpolbul.2017.01.006, 2017.

547   Bar-Or, I., Ben-Dov, E., Kushmaro, A., Eckert, W. and Sivan, O.: Methane-related changes in
548   prokaryotes along geochemical profiles in sediments of Lake Kinneret (Israel), Biogeosciences, 12,
549   2847–2860, doi:10.5194/bg-12-2847-2015, 2015.

550   Bar-Or, I., Elvert, M., Eckert, W., Kushmaro, A., Vigderovich, H., Zhu, Q., Ben-Dov, E. and Sivan, O.:
551   Iron-Coupled Anaerobic Oxidation of Methane Performed by a Mixed Bacterial-Archaeal Community
552   Based on Poorly Reactive Minerals, Environ. Sci. Technol., 51, 12293–12301,
553   doi:10.1021/acs.est.7b03126, 2017.

554   Bareket, M. M., Bookman, R., Katsman, R., de Stigter, H. and Herut, B.: The role of transport
555   processes of particulate mercury in modifying marine anthropogenic secondary sources, the case of
556   Haifa bay, Israel, Mar. Pollut. Bull., 105(1), 286–291, doi:10.1016/j.marpolbul.2016.02.014, 2016.

557   Beal, E. J., House, C. H. and Orphan, V. J.: Manganese-and Iron-Dependent Marine Methane
558   Oxidation, Science, 325(5937), 184–187, doi:10.1126/science.1169984, 2009.

559   Boetius, A., Ravenschlag, K., Schubert, C. J., Rickert, D., Widdel, F., Gieseke, A., Amann, R.,
560   Jùrgensen, B. B., Witte, U. and Pfannkuche, O.: A marine microbial consortium apparently mediating
561   anaerobic oxidation of methane, Lett. to Nat., 407(October), 623–626, 2000.

562   Bond, D. R. and Lovley, D. R.: Reduction of Fe (III) oxide by methanogens in the presence and
563   absence of extracellular quinones, Environ. Microbiol., 4(2), 115–124, doi:10.1046/j.1462-
564   2920.2002.00279.x, 2002.

565   Bond, P. L., Hugenholtz, P., Keller, J. and Blackall, L. L.: Bacterial Community Structures of
566   Phosphate-Removing and Non-Phosphate-Removing Activated Sludges from Sequencing Batch
567   Reactors, Appl. Environ. Microbial., 61(5), 1910–1916, 1995.

568   Bottrell, S. H., Parkes, R. J., Cragg, B. a. and Raiswell, R.: Isotopic evidence for anoxic pyrite
569   oxidation and stimulation of bacterial sulphate reduction in marine sediments, J. Geol. Soc. London.,

157(4), 711–714, doi:10.1144/jgs.157.4.711, 2000.

Bray, M. S., Jieying, W., Reed, B. C., Kretz, C. B., Belli, K. M., Simister, R. L., Henny, C., Stewart, F. J., DiChristina, T. J., Brandes, J. A., Fowle, D. A., Crowe, S. A. and Glass, J. B.: Shifting microbial communities sustain multi-year iron reduction and methanogenesis in ferruginous sediment incubations, Geobiology, doi:http://dx.doi.org/10.1101/087783., 2018.

Brunner, B., Arnold, G. L., Røy, H., Müller, I. A. and Jørgensen, B. B.: Off Limits : Sulfate below the Sulfate-Methane Transition, Front. earth Sci., 4(July), 1–16, doi:10.3389/feart.2016.00075, 2016.

Buongiorno, J., Turner, S., Webster, G., Asai, M., Shumaker, A. K., Roy, T., Weightman, A., Schippers, A. and Lloyd, K. G.: Interlaboratory quantification of Bacteria and Archaea in deeply buried sediments of the Baltic Sea (IODP Expedition 347), FEMS Microbiol. Ecol., (93), 1–16, doi:10.1093/femsec/fix007, 2017.

Cai, C., Leu, A. O., Jianhua, G. X., Yuexing, G., Zhao, F. J. and Tyson, G. W.: A methanotrophic archaeon couples anaerobic oxidation of methane to Fe (III) reduction, ISME J., 8(13), 1929–1939, doi:10.1038/s41396-018-0109-x, 2018.

Canfield, D. E.: Reactive iron in marine sediments, Geochim. Cosmochim. Acta, 53(3), 619–632, doi:10.1016/0016-7037(89)90005-7, 1989.

Caporaso, J. G., Kuczynski, J., Stombaugh, J., Bittinger, K., Bushman, F. D., Costello, E. K., Fierer, N., Peña, A. G., Goodrich, J. K., Gordon, J. I., Huttley, G. A., Kelley, S. T., Knights, D., Koenig, J. E., Ley, R. E., Lozupone, C. A., McDonald, D., Muegge, B. D., Pirrung, M., Reeder, J., Sevinsky, J. R., Turnbaugh, P. J., Walters, W. A., Widmann, J., Yatsunenko, T., Zaneveld, J. and Knight, R.: QIIME allows analysis of high-throughput com- munity sequencing data., Nat. Methods, (7), 335–336, doi:10.1038/nmeth.f.303, 2010.

Chen, W. H., Chen, S. Y., Kumar Khanal, S. and Sung, S.: Kinetic study of biological hydrogen production by anaerobic fermentation, Int. J. Hydrogen Energy, 31(15), 2170–2178, doi:10.4304/jcp.6.4.740-746, 2006.

Cline, J. D.: Spectrophotometric determination of hydrogen sulfide in natural waters, Limnol. Oceanogr., 454–458, doi:https://doi.org/10.4319/lo.1969.14.3.0454, 1969.

Conrad, R.: Contribution of hydrogen to methane production and control of hydrogen concentrations in methanogenic soils and sediments, FEMS Microbiol. Ecol., 28(3), 193–202, 1999.

Conrad, R.: Quantification of methanogenic pathways using stable carbon isotopic signatures : a review and a proposal, Org. Geochem., 36, 739–752, doi:10.1016/j.orggeochem.2004.09.006, 2005.

Conrad, R., Schink, B. and Phelps, T. J.: Thermodynamics of H_2-consuming and H_2-producing metabolic reactions in diverse methanogenic environments under in situ conditions, FEMS Microbiol. Ecol., 38, 353–360, 1986.

Coolen, M. J. L., Cypionka, H., Sass, A. M., Sass, H. and Overmann, J.: Ongoing modification of

Mediterranean pleistocene sapropels mediated by prokaryotes, Science, 296(June), 2407–2411, doi:10.1126/science.1071893, 2002.

Crowe, S. A., Katsev, S., Leslie, K., Sturm, A., Magen, C., Nomosatryo, S., Pack, M. A., Kessler, J. D., Reeburgh, W. S., Robert S, J. A., Gonzalez, L., Douglas Haffner, G., Mucci, A., Sundby, B. and Fowle, D.: The methane cycle in ferruginous Lake Matano, Geobiology, 9, 61–78, doi:10.1111/j.1472-4669.2010.00257.x, 2011.

Egger, M., Rasigraf, O., Sapart, C. J., Jilbert, T., Jetten, M. S. M., Röckmann, T., Van Der Veen, C., Bânda, N., Kartal, B., Ettwig, K. F. and Slomp, C. P.: Iron-mediated anaerobic oxidation of methane in brackish coastal sediments, Environ. Sci. Technol., 49(1), 277–283, doi:10.1021/es503663z, 2014.

Egger, M., Kraal, P., Jilbert, T., Sulu-Gambari, F., Sapart, C. J., Röckmann, T. and Slomp, C. P.: Anaerobic oxidation of methane alters diagenetic records of sulfur, iron and phosphorus in Black Sea sediments, Biogeosciences Discuss., (March), 1–39, doi:10.5194/bg-2016-64, 2016.

Egger, M., Hagens, M., Sapart, C. J., Dijkstra, N., van Helmond, N. A. G. M., Mogollón, J. M., Risgaard-Petersen, N., van der Veen, C., Kasten, S., Riedinger, N., Böttcher, M. E., Röckmann, T., Jørgensen, B. B. and Slomp, C. P.: Iron oxide reduction in methane-rich deep Baltic Sea sediments, Geochim. Cosmochim. Acta, 207, 256–276, doi:10.1016/j.gca.2017.03.019, 2017.

Emerson, S., Jahnke, R., Bender, M., Froelich, P. and Klinkhammer, G.: Early diagenesis in sediments from the eastern equatorial pacific, i. pore water nutrient and carbonate results, Earth Planet. Sci. Lett., 49, doi:https://doi.org/10.1016/0012-821X(80)90150-8, 1980.

Ettwig, K. F., Zhu, B., Speth, D., Keltjens, J. T., Jetten, M. S. M. and Kartal, B.: Archaea catalyze iron-dependent anaerobic oxidation of methane, Proc. Natl. Acad. Sci., 113(45), 12792–12796, doi:10.1073/pnas.1609534113, 2016.

Evans, P. N., Parks, D. H., Chadwick, G. L., Robbins, S. J., Orphan, V. J., Golding, S. D. and Tyson, G. W.: Methane metabolism in the archaeal phylum Bathyarchaeota revealed by genome-centric metagenomics, Science, 350(6259), 434–438, doi:10.1126/science.aac7745, 2015.

Feng, X., Wang, Y., Zubin, R. and Wang, F.: Core Metabolic Features and Hot Origin of Bathyarchaeota, Engineering, doi:10.1016/j.eng.2019.01.011, 2019.

Fischer, D., Mogollón, J. M., Strasser, M., Pape, T., Bohrmann, G., Fekete, N., Spiess, V. and Kasten, S.: Subduction zone earthquake as potential trigger of submarine hydrocarbon seepage, Nat. Geosci., 6(8), 1–5, doi:10.1038/ngeo1886, 2013.

Froelich, P. N., Klinkhammer, G. P., Bender, M. L., Luedtke, N. A., Heath, G. R., Cullen, D., Dauphin, P., Hammond, D., Hartman, B. and Maynard, V.: Early oxidation of organic matter in pelagic sediments of the eastern equatorial Atlantic: Suboxic diagenesis, Geochim. Cosmochim. Acta, 43, 1075–1090, doi:https://doi.org/10.1016/0016-7037(79)90095-4, 1979.

He, Y., Li, M., Perumal, V., Feng, X., Fang, J., Xie, J., Sievert, S. M. and Wang, F.: Genomic and

enzymatic evidence for acetogenesis among multiple lineages of the archaeal phylum Bathyarchaeota widespread in marine sediments, Nat. Microbiol., (April), 1–9, doi:10.1038/nmicrobiol.2016.35, 2016.

Herut, B., Almogi-Labin, A., Jannink, N. and Gertman, I.: The seasonal dynamics of nutrient and chlorophyll a concentrations on the SE Mediterranean shelf-slope, Oceanol. Acta, 23(7), 771–782, doi:10.1016/S0399-1784(00)01118-X, 2000.

Hinrichs, K., Hayes, J. M. and Sylva, S. P.: Methane-consuming archaebacteria in marine sediments, Lett. to Nat., 398(April), 802–805, 1999.

Hoehler, T. M., Alperin, M. J., Albert, D. B. and Martens, C. S.: Field and laboratory studies of methane oxidation in an anoxic marine sediment: evidence for a methanogen-sulfate reducer consortium, Global Biogeochem. Cycles, 8(4), 451–463, doi:https://doi.org/10.1029/94GB01800, 1994.

Holler, T., Wegener, G., Knittel, K., Boetius, A., Brunner, B., Kuypers, M. M. M. and Widdel, F.: Substantial 13 C / 12 C and D / H fractionation during anaerobic oxidation of methane by marine consortia enriched in vitro, Environ. Microbiol. Reports., 1, 370–376, doi:10.1111/j.1758-2229.2009.00074.x, 2009.

Holmkvist, L., Ferdelman, T. G. and Jørgensen, B. B.: A cryptic sulfur cycle driven by iron in the methane zone of marine sediment (Aarhus Bay, Denmark), Geochim. Cosmochim. Acta, 75(12), 3581–3599, doi:10.1016/j.gca.2011.03.033, 2011.

Iversen, N. and Jørgensen, B. B.: Anaerobic methane oxidation rates at the sulfate-methane transition in marine sediments from Kattegat and Skagerrak (Denmark), Limnol. Oceanogr., 1983(5), 944–955, 1985.

Jørgensen, B. B., Böttcher, M. E., Lüschen, H., Neretin, L. N. and Volkov, I. I.: Anaerobic methane oxidation and a deep H 2 S sink generate isotopically heavy sulfides in Black Sea sediments, Geochim. Cosmochim. Acta, 68(9), 2095–2118, doi:10.1016/j.gca.2003.07.017, 2004.

Kawaichi, S., Ito, N., Kamikawa, R., Sugawara, T., Yoshida, T. and Sako, Y.: Ardenticatena maritima gen. nov., sp. nov., a ferric iron- and nitrate-reducing bacterium of the phylum 'Chloroflexi' isolated from an iron-rich coastal hydrothermal field, and description of Ardenticatenia classis nov., Int. J. Syst. Evol. Microbiol., (63), 2992–3002, doi:10.1099/ijs.0.046532-0, 2013.

Knittel, K. and Boetius, A.: Anaerobic Oxidation of Methane : Progress with an Unknown Process, Annu. Rev. Microbiol., 63, 311–334, doi:10.1146/annurev.micro.61.080706.093130, 2009.

Kress, N. and Herut, B.: Spatial and seasonal evolution of dissolved oxygen and nutrients in the Southern Levantine Basin (Eastern Mediterranean Sea): chemical characterization of the water masses and inferences on the N : P ratios, Deep Sea Research Part I: Oceanographic Research Papers, 48, 2347–2372, doi:10.1016/S0967-0637(01)00022-X, 2001.

Kulichevskaya, I. S., Suzina, N. E., Rijpstra, W. I. C., Dedysh, S. N. and Damste, J. S. S.: a facultative anaerobe capable of dissimilatory iron reduction from subdivision 3 of the Acidobacteria, Int. J. Syst.

675   Evol. Microbiol., (64), 2857–2864, doi:10.1099/ijs.0.066175-0, 2014.

676   Li, Y., Yu, S., Strong, J. and Wang, H.: Are the biogeochemical cycles of carbon , nitrogen , sulfur ,

677   and phosphorus driven by the " Fe III – Fe II redox wheel " in dynamic redox environments ?, J. soils

678   sediments, 12(5), 683–693, doi:10.1007/s11368-012-0507-z, 2012.

679   Lilley, M. D., Baross, J. A. and Gordon, L. I.: Dissolved hydrogen and methane in Saanich Inlet,

680   British Columbia, Deep Sea Res. Part A, Oceanogr. Res. Pap., 29(12), 1471–1484, doi:10.1016/0198-

681   0149(82)90037-1, 1982.

682   Liu, D., Dong Hailiang, H., Bishop, M. E., Wang, H., Agrawal, A., Tritschler, S., Eberl, D. D. and Xie,

683   S.: Reduction of structural Fe(III) in nontronite by methanogen Methanosarcina barkeri, Geochim.

684   Cosmochim. Acta, 75(4), 1057–1071, doi:10.1016/j.gca.2010.11.009, 2011.

685   Lloyd, K. G., Schreiber, L., Petersen, D. G., Kjeldsen, K. U., Lever, M. A., Steen, A. D., Stepanauskas,

686   R., Richter, M., Kleindienst, S., Lenk, S., Schramm, A. and Jørgensen, B. B.: Predominant archaea in

687   marine sediments degrade detrital proteins, Nature, 496(7444), 215–218, doi:10.1038/nature12033,

688   2013.

689   Lovley, D. R. and Goodwin, S.: Hydrogen concentrations as an indicator of the predominant terminal

690   electron-accepting reactions in aquatic sediments, Geochim. Cosmochim. Acta, 52, 2993–3003,

691   doi:10.1016/0016-7037(88)90163-9, 1988.

692   Lovley, D.: Microbial Fe (III) reduction in subsurface environments, FEMS Microbiol. Rev., 20, 305–

693   313, doi:10.1111/j.1574-6976.1997.tb00316.x/full, 1997.

694   Lovley, D. R.: Dissimilatory Fe(III) and Mn(IV) reduction., Microbiol. Rev., 55(2), 259–287, 1991.

695   Lovley, D. R. and Phillips, E. J.: Novel mode of microbial energy metabolism: organic carbon

696   oxidation coupled to dissimilatory reduction of iron or manganese., Appl. Environ. Microbiol., 54(6),

697   1472–1480, doi:10.1103/PhysRevLett.50.1998, 1988.

698   Lovley, D. R. and Phillips, E. J. P.: Organic matter mineralization with reduction of ferric iron in

699   anaerobic sediments., Appl. Environ. Microbiol., 51(4), 683–689, doi:10.1080/01490458709385975,

700   1986.

701   Lovley, D. R., Stolz, J. F., Nord, G. L. and Phillips, E. J. P.: Anaerobic production of magnetite by a

702   dissimilatory iron-reducing microorganism, Nature, 330(6145), 252–254, doi:10.1038/330252a0, 1987.

703   Lovley, D. R., Coates, J. D., BluntHarris, E. L., Phillips, E. J. P. and Woodward, J. C.: Humic

704   substances as electron acceptors for microbial respiration, Nature, 382(6590), 445–448,

705   doi:10.1038/382445a0, 1996.

706   März, C., Hoffmann, J., Bleil, U., Lange, G. J. De and Kasten, S.: Diagenetic changes of magnetic and

707   geochemical signals by anaerobic methane oxidation in sediments of the Zambezi deep-sea fan (SW

708   Indian Ocean), Mar. Geol., 255(3–4), 118–130, doi:10.1016/j.margeo.2008.05.013, 2008.

709   März, C., Riedinger, N., Sena, C. and Kasten, S.: Phosphorus dynamics around the sulphate-methane

710   transition in continental margin sediments : Authigenic apatite and Fe (II) phosphates, Mar. Geol.,

711   404(July), 84–96, doi:10.1016/j.margeo.2018.07.010, 2018.

712   McGlynn, S. E., Chadwick, G. L., Kempes, C. P. and Orphan, V. J.: Single cell activity reveals direct

713   electron transfer in methanotrophic consortia, Nature, 526(7574), 531–535,

714   doi:doi:10.1038/nature15512, 2015.

715   Meng, J., Xu, J., Qin, D., He, Y., Xiao, X. and Wang, F.: Genetic and functional properties of

716   uncultivated MCG archaea assessed by metagenome and gene expression analyses, ISME J., 8(3), 650–

717   9, doi:10.1038/ismej.2013.174, 2014.

718   Milkov, A. V: Global estimates of hydrate-bound gas in marine sediments : how much is really out

719   there?, Earth-Science Rev., 66, 183–197, doi:10.1016/j.earscirev.2003.11.002, 2004.

720   Milkov, A. V and Sassen, R.: Economic geology of offshore gas hydrate accumulations and provinces,

721   Mar. Pet. Geol., 19, 1–11, doi:doi.org/10.1016/S0264-8172(01)00047-2, 2002.

722   Mountfort, D. O. and Asher, R. A.: Role of Sulfate Reduction Versus Methanogenesis in Terminal

723   Carbon Flow in Polluted Intertidal Sediment of Waimea Inlet, Nelson, New Zealand, Appl. Environ.

724   Microbiol., 42(2), 252–258, doi:0099-2240/81/080252-07$02.00/0, 1981.

725   Mountfort, D. O., Asher, R. a, Mays, E. L. and Tiedje, J. M.: Carbon and electron flow in mud and

726   sandflat intertidal sediments at delaware inlet, nelson, new zealand., Appl. Environ. Microbiol., 39(4),

727   686–94, doi:0099-2240/80/04-0686/09$02.00/0, 1980.

728   Moutin, T. and Raimbault, P.: Primary production , carbon export and nutrients availability in western

729   and eastern Mediterranean Sea in early summer 1996 (MINOS cruise), J. Mar. Syst., 34, 273–288,

730   doi:doi.org/10.1016/S0924-7963(02)00062-3, 2002.

731   Neiwöhner, C., Hensen, C., Kasten, S., Zabel, M. and Schulz, H. D.: Deep sulfate reduction completely

732   mediated by anaerobic methane oxidation in sediments of the upwelling area off Namibia,

733   Geochim.Cosmochim.Acta, 62(3), 455–464, 1998.

734   Nir, Y.: Recent sediments of the Israel Mediterranean continental shelf and slope, University of

735   Gothenburg. http://hdl.handle.net/2077/13267, 1984.

736   Niu, M., Fan, X., Zhuang, G., Liang, Q. and Wang, F.: Methane-metabolizing microbial communities

737   in sediments of the Haima cold seep area , northwest slope of the South China Sea, FEMS Microbiol.

738   Ecol., (March), 1–13, doi:10.1093/femsec/fix101, 2017.

739   Norði, K. Á., Thamdrup, B. and Schubert, C. J.: Anaerobic oxidation of methane in an iron-rich Danish

740   freshwater lake sediment, Limnol. Oceanogr., 58(2), 546–554, doi:10.4319/lo.2013.58.2.0546, 2013.

741   Novelli, P. C., Scranton, M. I. and Michener, R. H.: Hydrogen Distributions in Marine Sediments

742   Hydrogen distributions, Limnol. Oceanogr., 32(3), 565–576, doi:10.4319/lo.1987.32.3.0565, 1987.

743 Nüsslein, B., Eckert, W. and Conrad, R.: Stable isotope biogeochemistry of methane formation in

744 profundal sediments of Lake Kinneret (Israel), Limnol. Oceanogr., 48(4), 1439–1446,

745 doi:10.4319/lo.2003.48.4.1439, 2003.

746 Oni, O., Miyatake, T., Kasten, S., Richter-Heitmann, T., Fischer, D., Wagenknecht, Laura Kulkarni, A.,

747 Blumers, M., Shylin, S. I., Ksenofontov, Vadim Costa, B. F. O., Klingelhöfer, G. and Friedrich, M. W.:

748 Distinct microbial populations are tightly linked to the profile of dissolved iron in the methanic

749 sediments of the Helgoland mud area , North Sea, Front. Microbiol., 6(May), 1–15,

750 doi:10.3389/fmicb.2015.00365, 2015.

751 Orphan, V. J., House, C. H. and Hinrichs, K.: Methane-Consuming Archaea Revealed by Directly

752 Coupled Isotopic and Phylogenetic Analysis, Science, 293(July), 484–488,

753 doi:10.1126/science.1061338, 2001.

754 Paull, C. K., Normark, W. R., Ussler, W., Caress, D. W. and Keaten, R.: Association among active

755 seafloor deformation , mound formation , and gas hydrate growth and accumulation within the seafloor

756 of the Santa Monica Basin , offshore California, Mar. Geol., 250, 258–275,

757 doi:10.1016/j.margeo.2008.01.011, 2008.

758 Poulton, S. W. and Canfield, D. E.: Development of a sequential extraction procedure for iron:

759 Implications for iron partitioning in continentally derived particulates, Chem. Geol., 214(3–4), 209–

760 221, doi:10.1016/j.chemgeo.2004.09.003, 2005.

761 Poulton, S. W., Krom, M. D. and Raiswell, R.: A revised scheme for the reactivity of iron

762 (oxyhydr)oxide minerals towards dissolved sulfide, Geochim. Cosmochim. Acta, 68(18), 3703–3715,

763 doi:10.1016/j.gca.2004.03.012, 2004.

764 Riedinger, N., Pfeifer, K., Kasten, S., Garming, J. F. L., Vogt, C. and Hensen, C.: Diagenetic

765 alterations of magnetic signals by anaerobic oxidation of methane related to a change in sedimentation

766 rate, Geochim.Cosmochim.Acta, 69(16), 4117–4126, doi:10.1016/j.gca.2005.02.004, 2005.

767 Riedinger, N., Formolo, M. J., Lyons, T. W., Henkel, S., Beck, A. and Kasten, S.: An inorganic

768 geochemical argument for coupled anaerobic oxidation of methane and iron reduction in marine

769 sediments., Geobiology, 12(2), 172–81, 2014.

770 Riedinger, N., Brunner, B., Krastel, S., Arnold, G. L., Wehrmann, L. M., Formolo, M. J., Beck, A.,

771 Bates, S. M., Henkel, S., Kasten, S. and Lyons, T. W.: Sulfur Cycling in an Iron Oxide-Dominated ,

772 Dynamic Marine Depositional System : The Argentine Continental Margin, Front. earth Sci., 5(May),

773 doi:10.3389/feart.2017.00033, 2017.

774 Roden, E. E.: Fe(III) Oxide Reactivity Toward Biological versus Chemical Reduction, Environ. Sci.

775 Technol., 37(7), 1319–1324, doi:10.1021/es026038o, 2003.

776 Roden, E. E.: Geochemical and microbiological controls on dissimilatory iron reduction, Comptes

777 Rendus - Geosci., 338(6–7), 456–467, doi:10.1016/j.crte.2006.04.009, 2006.

778   Roden, E. E. and Wetzel, R. G.: Organic carbon oxidation and suppression of methane production by

779   microbial Fe(III) oxide reduction in vegetated and unvegetated freshwater wetland sediments, Limnol.

780   Oceanogr., 41(8), 1733–1748, doi:10.4319/lo.1996.41.8.1733, 1996.

781   Roden, E. E. and Wetzel, R. G.: Kinetics of microbial Fe (III) oxide reduction in freshwater wetland

782   sediments, Limnol. Ocean., 47(1), 198–211, doi:10.4319/lo.2002.47.1.0198, 2002.

783   Rooze, J., Egger, M., Tsandev, I. and Slomp, C. P.: Iron-dependent anaerobic oxidation of methane in

784   coastal surface sediments: potential controls and impact, Limnol. Oceanogr., (1),

785   doi:10.1002/lno.10275, 2016.

786   Rotaru, B. A. and Thamdrup, B.: A new diet for methane oxidizers, Biogeochemistry, 351(6274), 658–

787   660, doi:10.1126/science.aaf0741, 2016.

788   Salem, D. M. S. A., Khaled, A. and Nemr, A. El: Assessment of pesticides and polychlorinated

789   biphenyls (PCBs) in sediments of the Egyptian Mediterranean Coast, Egypt. J. Aquat. Res., 39(3),

790   141–152, doi:10.1016/j.ejar.2013.11.001, 2013.

791   Sandler, A. and Herut, B.: Composition of clays along the continental shelf off Israel: Contribution of

792   the Nile versus local sources, Mar. Geol., 167(3–4), 339–354, doi:10.1016/S0025-3227(00)00021-9,

793   2000.

794   Schattner, U., Lazar, M., Harari, D. and Waldmann, N.: Active gas migration systems offshore northern

795   Israel, first evidence from seafloor and subsurface data, Cont. Shelf Res., 48, 167–172,

796   doi:10.1016/j.csr.2012.08.003, 2012.

797   Scheller, S., Yu, H., Chadwick, G. L., McGlynn, S. E. and Orphan, V. J.: Artificial electron acceptors

798   decouple archaeal methane oxidation from sulfate reduction, Science, 351(6274), 1754–1756,

799   doi:10.1126/science.aad7154, 2016.

800   Segarra, K. E. a, Comerford, C., Slaughter, J. and Joye, S. B.: Impact of electron acceptor availability

801   on the anaerobic oxidation of methane in coastal freshwater and brackish wetland sediments, Geochim.

802   Cosmochim. Acta, 115, 15–30, doi:10.1016/j.gca.2013.03.029, 2013.

803   Sela-Adler, M., Herut, B., Bar-Or, I., Antler, G., Eliani-Russak, E., Levy, E., Makovsky, Y. and Sivan,

804   O.: Geochemical evidence for biogenic methane production and consumption in the shallow sediments

805   of the SE Mediterranean shelf (Israel), Cont. Shelf Res., 101, 117–124, doi:10.1016/j.csr.2015.04.001,

806   2015.

807   Sivan, O., Schrag, D. P. and Murray, R. W.: Rates of methanogenesis and methanotrophy in deep-sea

808   sediments, Geobiology, 5(2), 141–151, doi:10.1111/j.1472-4669.2007.00098.x, 2007.

809   Sivan, O., Adler, M., Pearson, A., Gelman, F., Bar-Or, I., John, S. G. and Eckert, W.: Geochemical

810   evidence for iron-mediated anaerobic oxidation of methane, Limnol. Oceanogr., 56(4), 1536–1544,

811   doi:10.4319/lo.2011.56.4.1536, 2011.

812   Sivan, O., Antler, G., Turchyn, A. V., Marlow, J. J. and Orphan, V. J.: Iron oxides stimulate sulfate-

driven anaerobic methane oxidation in seeps, Proc. Natl. Acad. Sci., 111, E4139–E4147, doi:10.1073/pnas.1412269111, 2014.

Sivan, O., Shusta, S. and Valentine, D. L.: Methanogens rapidly transition from methane production to iron reduction, Geobiology, 190–203, doi:10.1111/gbi.12172, 2016.

Slomp, C. P., Mort, H. P., Jilbert, T., Reed, D. C., Gustafsson, B. G. and Wolthers, M.: Coupled Dynamics of Iron and Phosphorus in Sediments of an Oligotrophic Coastal Basin and the Impact of Anaerobic Oxidation of Methane, Plos One, 8(4), doi:10.1371/journal.pone.0062386, 2013.

Song, Z., Wang, F., Zhi, X., Chen, J., Zhou, E., Liang, F., Xiao, X., Tang, S., Jiang, H., Zhang, C. L., Dong, H. and Li, W.: Bacterial and archaeal diversities in Yunnan and Tibetan hot springs , China, Environ. Microbiol., 15, 1160–1175, doi:10.1111/1462-2920.12025, 2013.

Stookey, L. L.: Ferrozine-a new spectrophotometric reagent for iron, Anal. Chem., 42(7), 779–781, doi:10.1021/ac60289a016, 1970.

Tan, S., Liu, J., Fang, Y., Hedlund, B. P., Lian, Z., Li, L. H. J., Li, L. H. W., Dong, H. J. H. and Shu, W.: Insights into ecological role of a new deltaproteobacterial order Candidatus Acidulodesulfobacterales by metagenomics and metatranscriptomics, ISME J., doi:10.1038/s41396-019-0415-y, 2019.

Treude, T., Krause, S., Maltby, J., Dale, A. W., Coffin, R. and Hamdan, L. J.: Sulfate reduction and methane oxidation activity below the sulfate-methane transition zone in Alaskan Beaufort Sea continental margin sediments: Implications for deep sulfur cycling, Geochim. Cosmochim. Acta, 144, 217–237, doi:10.1016/j.gca.2014.08.018, 2014.

Valentine, D. L.: Biogeochemistry and microbial ecology of methane oxidation in anoxic environments: A review, Antonie van Leeuwenhoek, Int. J. Gen. Mol. Microbiol., 81, 271–282, doi:10.1023/A:1020587206351, 2002.

Walters, W., Hyde, E. R., Berg-lyons, D., Ackermann, G., Humphrey, G., Parada, A., Gilbert, J. A. and Jansson, J. K.: Transcribed Spacer Marker Gene Primers for Microbial Community Surveys, Am. Soc. Microbiol., 1(1), 1–10, doi:10.1128/mSystems.00009-15, 2015.

Wang, Z., Guo, F., Liu, L. and Zhang, T.: Evidence of Carbon Fixation Pathway in a Bacterium from Candidate Phylum SBR1093 Revealed with Genomic Analysis, Plos One, 9(10), doi:10.1371/journal.pone.0109571, 2014.

Weber, K. A., Urrutia, M. M., Churchill, P. F., Kukkadapu, R. K. and Roden, E. E.: Anaerobic redox cycling of iron by freshwater sediment microorganisms, Environ. Microbiol., 8(1), 100–113, doi:10.1111/j.1462-2920.2005.00873.x, 2006.

Whiticar, M. J.: Carbon and hydrogen isotope systematics of bacterial formation and oxidation of methane, Chem. Geol., 161(1–3), 291–314, doi:10.1016/S0009-2541(99)00092-3, 1999.

Wurgaft, E., Findlay, A. J., Vigderovich, H., Herut, B. and Sivan, O.: Sulfate reduction rates in the

848   sediments of the Mediterranean continental shelf inferred from combined dissolved inorganic carbon

849   and total alkalinity profiles, Mar. Chem., 211, 64–74, doi:10.1016/j.marchem.2019.03.004, 2019.

850   Yan, Z., Joshi, P., Gorski, C. A. and Ferry, J. G.: A biochemical framework for anaerobic oxidation of

851   methane driven by Fe(III)-dependent respiration, Nat. Commun., (Iii), 1–9, doi:10.1038/s41467-018-

852   04097-9, 2018.

853   Yu, T., Wu, W., Liang, W., Alexander, M. and Hinrichs, K.: Growth of sedimentary Bathyarchaeota on

854   lignin as an energy source, Proc. Natl. Acad. Sci., 115(23), 6022–6027, doi:10.1073/pnas.1718854115,

855   2018.

856   Zehnder, a. J. B. and Brock, T. D.: Anaerobic methane oxidation: Occurrence and ecology, Appl.

857   Environ. Microbiol., 39(1), 194–204, http://aem.asm.org/content/39/1/194, 1980.

858   Zhang, C. L. and Lanoil, B.: Geomicrobiology and biogeochemistry of gas hydrates and cold seeps,

859   Chemocal Geol., 205, 187–194, doi:10.1016/j.chemgeo.2004.01.001, 2004.

860   Zhang, J., Dong, H., Liu, D., Fischer, T. B., Wang, S. and Huang, L.: Microbial reduction of Fe(III) in

861   illite–smectite minerals by methanogen Methanosarcina mazei, Chem. Geol., 292–293, 35–44,

862   doi:10.1016/j.chemgeo.2011.11.003, 2012.

863   Zhang, J., Dong, H., Liu, D. and Agrawal, A.: Microbial reduction of Fe(III) in smectite minerals by

864   thermophilic methanogen Methanothermobacter thermautotrophicus, Geochim. Cosmochim. Acta, 106,

865   203–215, doi:10.1016/j.gca.2012.12.031, 2013.

866   Zhou, Z., Pan, J., Wang, F., Gu, J. and Li, M.: Bathyarchaeota : globally distributed metabolic

867   generalists in anoxic environments, FEMS Microbiol. Rev., (May), 639–655,

868   doi:10.1093/femsre/fuy023, 2018.

869

870

871   **Table 1**: Cores sampling details: dates, water depths and locations.

Date	station	water depth (m)	Latitude	Longtitude
August 14, 2013	PC-5	87	32°55.47'	34°54.01'
	PC-3	81	32°55.29'	34°54.14'
February 6, 2014	PC-3	82	32°55.30'	34°54.14'
January, 2015	PC-3	82	32°55.30'	34°54.14'
June 9, 2015	SG-1	89	32°57.87'	34°55.30'
September 17, 2015	SG-1	84	32°57.91'	34°55.27'
January 24, 2017	SG-1	85	32°57.51'	34°55.15'

872

873   **Table 2**: Experimental set-up of the slurry incubation experiment.

Treatment	Number of bottles
Hematite	2
Magnetite	2
Hematite + H$_2$	2
Magnetite + H$_2$	3
Killed + hematite + H$_2$	2
Killed + magnetite + H$_2$	1

874

875   **Table 3**: Summary of reactive iron extraction procedure (after Poulton and Canfield, 2005).

Extractant	Target compounds	Analyzed species	Formula	Shaking time (h)
Magnesium chloride	Ion-exchangeble Fe(II)	Adsorbed ferrous iron	Fe^{2+}	2
Sodium acetate	Iron carbonates	Siderite Ankerite	$FeCO_3$ $Ca(Fe^{+2},Mg^{+2},Mn^{+2})(CO_3)_2$	24
Hydroxylamine hydrochloride	"Easily reducible" Iron(hydr)oxides	Ferrihydrite, Lepidicrocite	$Fe^{3+}_2O_3*0.5(H_2O)$ γ-$FeOOH$	48
Sodium dithionite	"Reducible" oxides	Goethite, Hematite, Akageneite	α-$FeOOH$ Fe_2O_3 β-$FeOOH$	2
Ammonium oxalate	Poorly crystalline	Magnetite	Fe_3O_4	6

876

877   **Figures captions:**

Figure 1: A map of the study area with the location of the three stations that were sampled SG-1, PC-3 and PC-5 (after Wurgaft et al., 2019).

878   **Figure 2**: Geochemical pore-water profiles of: total S, CH_4, $\delta^{13}C_{DIC}$, dissolved Fe(II), H_2 and extractable Fe fractions from sediment cores collected at the two stations: SG-1 (a-f) and PC-3 (g-l) in the SE Mediterranean. The profiles are divided roughly into three zones according to the dominant processes: upper microbial iron and sulfate reduction, sulfate-methane transition zone (SMTZ), and the methanic zone at the deep part. The dashed line in the CH_4 graph at SG-1 station represents the CH_4 saturation value in the pore-water (Sela-Adler et al., 2015). The following extractable Fe fraction profiles of stations SG-1 (f) and PC-3 (l) are from the September 2015 and January 2015 cruise (respectively): Fe_{carb} (●), Fe_{ox1} (■) Feo_{x2} (▲), Fe_{mag} (▼), Fe_{py} (◆) (Wurgaft et al., 2019) and total reactive iron (●). The error bars for CH_4 are presented where duplicate sediment samples were collected. The error bars for Fe(II), $\delta^{13}C_{DIC}$ and H_2 are presented where measurements from the same sample were repeated at least twice. The analytical errors were too small to be displayed.

Figure 3: Sedimentary depth profiles of bacterial and archaeal 16S rRNA and *mcrA* functional genes of station SG-1 from January 2017, divided to three zones (as described in figure 2). Triplicates were produced from each sample with error bars smaller than the symbols displayed.

Figure 4: Phyla level classification of bacterial (a) and archaeal (b) diversity in the sediments of Station SG-1 from January 2017.

Figure 5: Dissolved Fe(II) results of the sediment slurry incubation experiment. The sediment was collected from Station SG-1 on January 2017 from sediment depth of 265-285 cm. The error bars were smaller than the symbols displayed.

Figure 6: The relationship between dissolved Fe(II) concentrations and methane concentrations in zone 3 of (a) Station SG-1 and (b) Station PC-3. An inverse association is observed between the two species, suggesting a relationship of competition or iron-coupled AOM.

879 **Figures**:

880 **Figure 1**

881

911   **Figure 2**

912

913
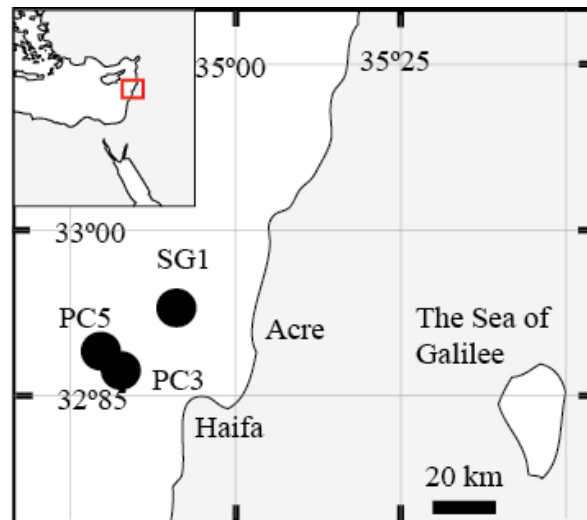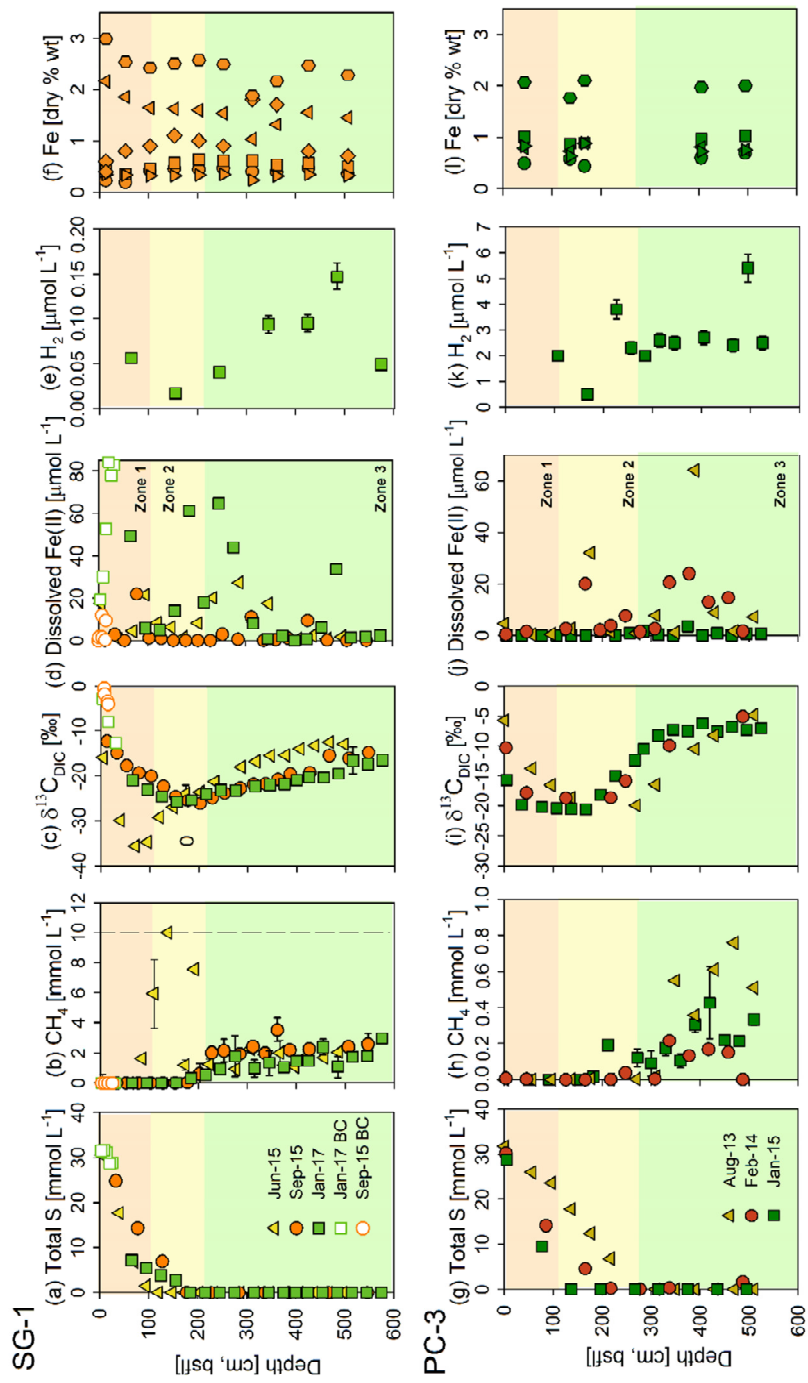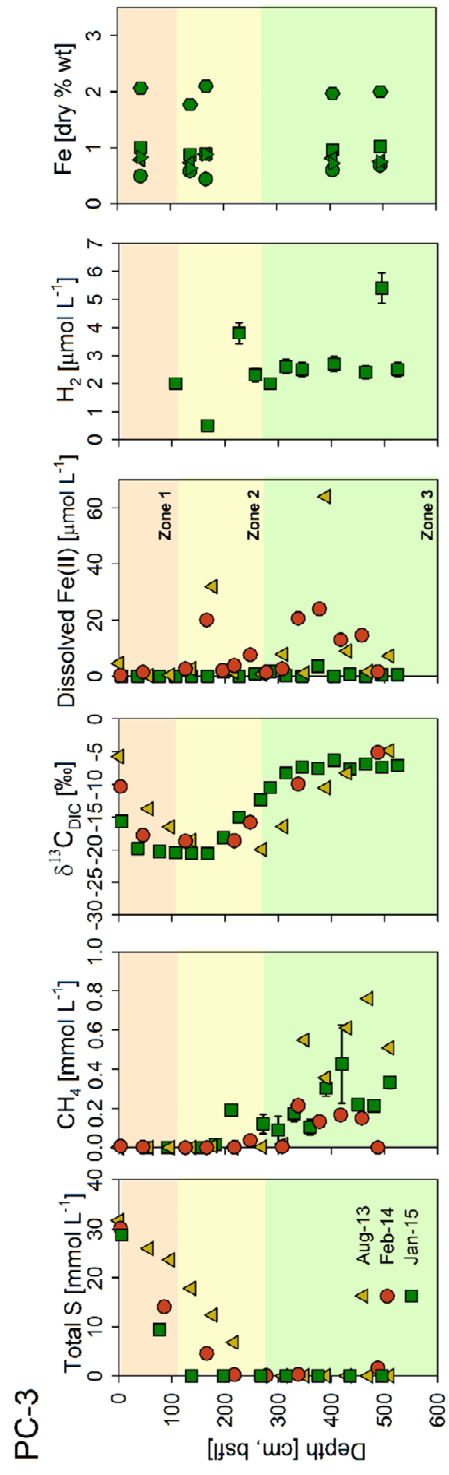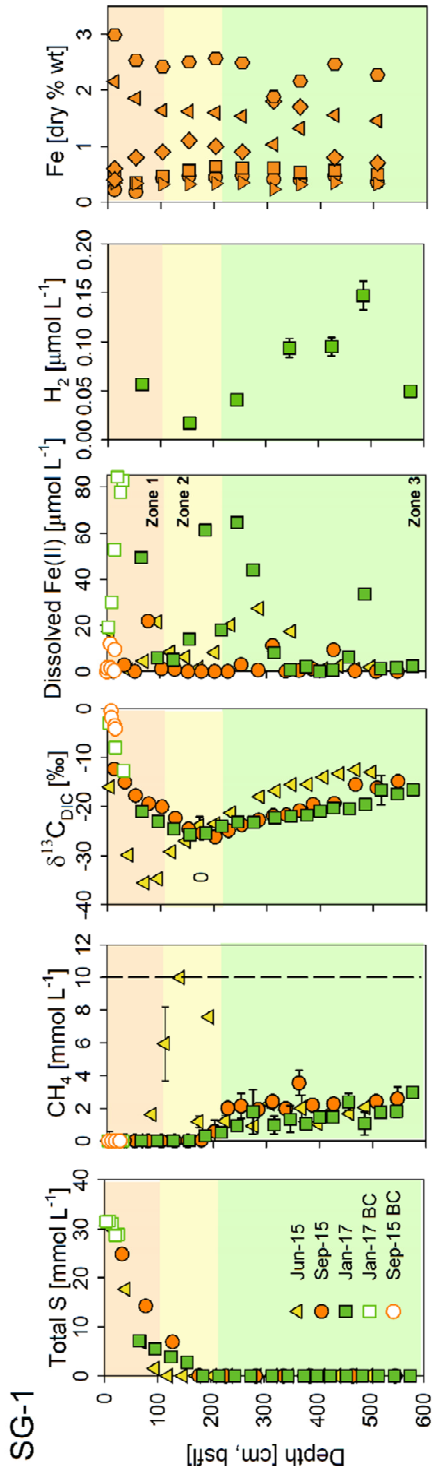
919 **Figure 3**

920

921
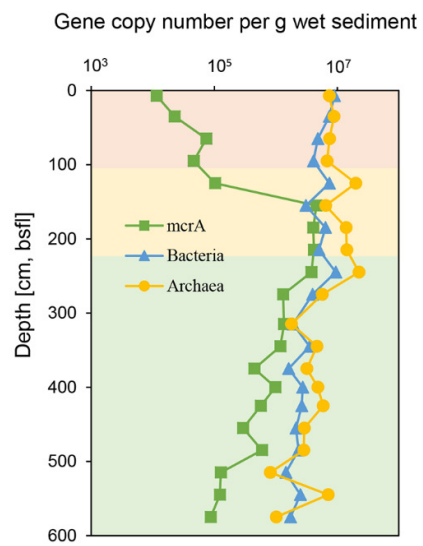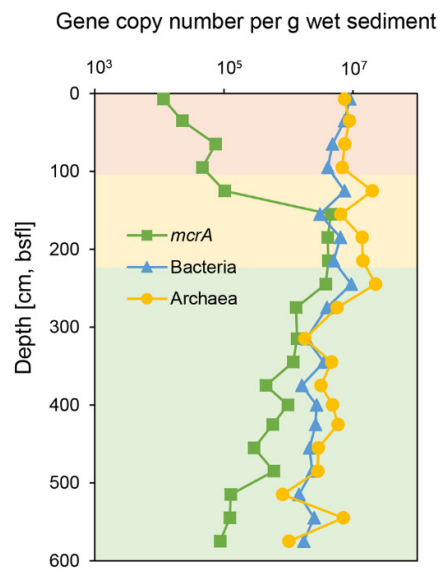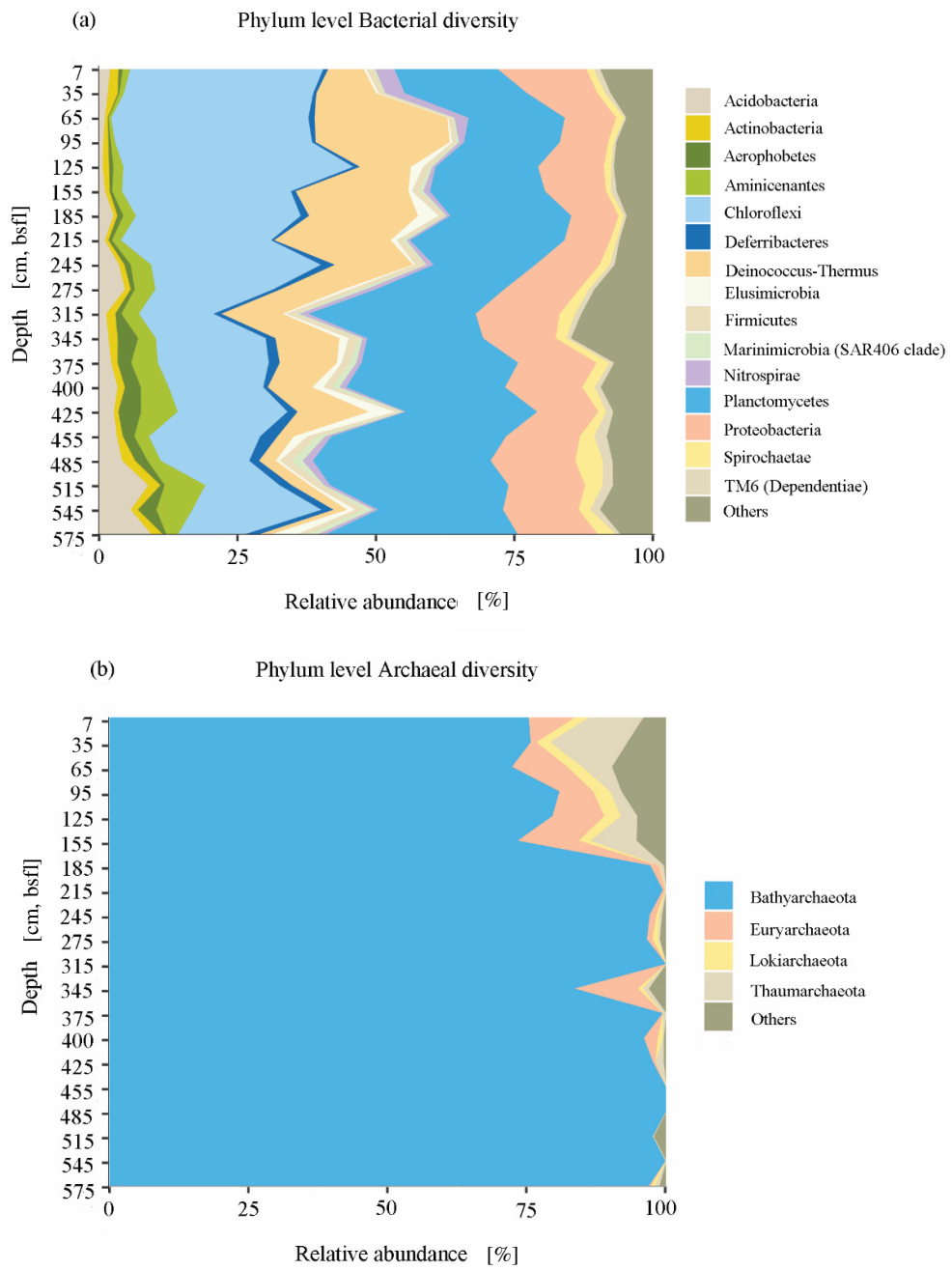
 Figure 4

928   **Figure 5**
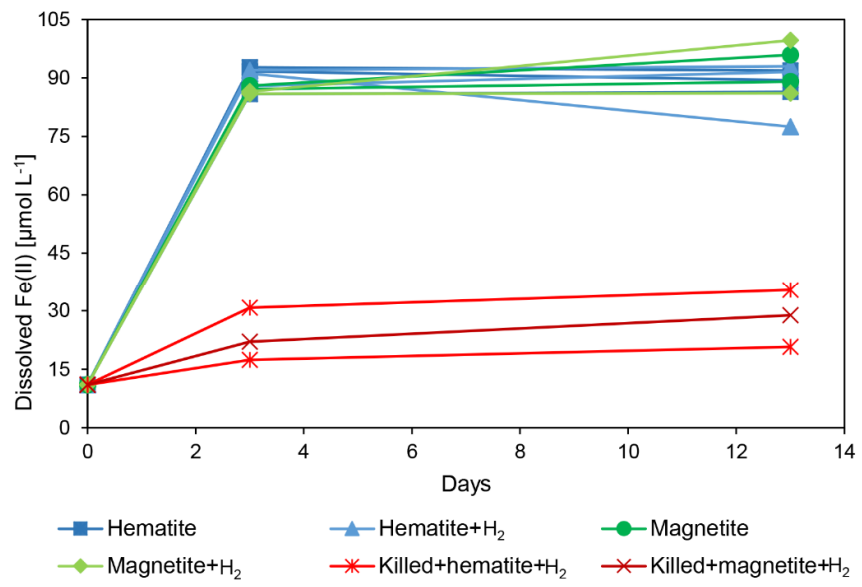
929

930

931   **Figure 6**
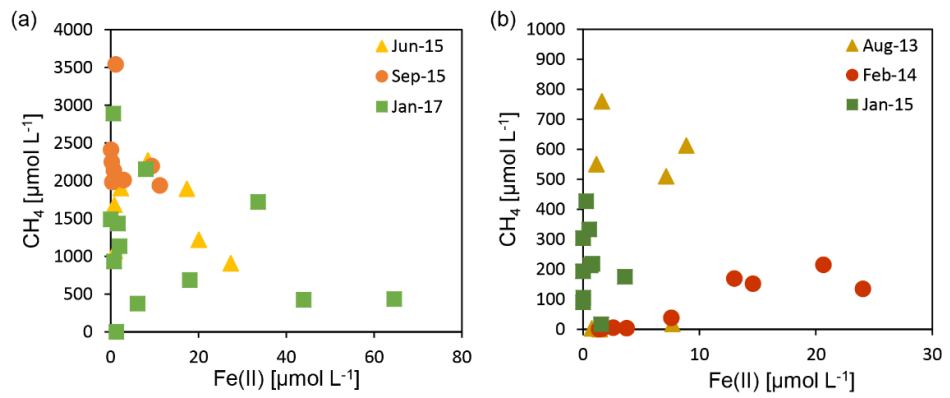
932

933

934

935

936

937

938

939